

EUR 3752 e

EUROPEAN ATOMIC ENERGY COMMUNITY - EURATOM

**RESEARCH TO DETERMINE THE LONG-TERM MECHANICAL
PROPERTIES OF METALS SUBJECTED TO MECHANICAL STRESS
AT ELEVATED TEMPERATURES AND NEUTRON IRRADIATION**

Final Report

by

**W. SIEGFRIED and S. ZIMERING
(Battelle Memorial Institute)**

1968



**EURATOM/US Agreement for Cooperation
EURAEK Report No. 1921 prepared by the
Battelle Memorial Institute, Geneva - Switzerland**

**Euratom Contracts No. 100-62-12 RDS
and No. 057-64-7 TEES**

LEGAL NOTICE

This document was prepared under the sponsorship of the Commission of the European Communities in pursuance of the joint programme laid down by the Agreement for Cooperation signed on 8 November 1958 between the Government of the United States of America and the European Communities.

It is specified that neither the Commission of the European Communities, nor the Government of the United States, their contractors or any person acting on their behalf :

Make any warranty or representation, express or implied, with respect to the accuracy, completeness, or usefulness of the information contained in this document, or that the use of any information, apparatus, method, or process disclosed in this document may not infringe privately owned rights; or

Assume any liability with respect to the use of, or for damages resulting from the use of any information, apparatus, method or process disclosed in this document.

This report is on sale at the addresses listed on cover page 4

at the price of FF 10.—	FB 100.—	DM 8.—	Lit. 1.250	Fl. 7.25
-------------------------	----------	--------	------------	----------

When ordering, please quote the EUR number and the title, which are indicated on the cover of each report.

Printed by SMEETS
Brussels, April 1968

This document was reproduced on the basis of the best available copy.

EUR 3752 e

RESEARCH TO DETERMINE THE LONG-TERM MECHANICAL PROPERTIES OF METALS SUBJECTED TO MECHANICAL STRESS AT ELEVATED TEMPERATURES AND NEUTRON IRRADIATION - Final Report by W. SIEGFRIED and S. ZIMERING (Battelle Memorial Institute)

European Atomic Energy Community - EURATOM
EURATOM/US Agreement for Cooperation
EURAEC Report No. 1921 prepared by the Battelle Memorial Institute, Geneva (Switzerland)
Euratom Contracts No. 100-62-12 RDS and No. 057-64-7 TEES
Brussels, April 1968 - 68 Pages - 26 Figures - FB 100

Improvement of the determination of long-time mechanical properties of metals stressed at high temperature under irradiation is studied by means of solid state physics.

EUR 3752 e

RESEARCH TO DETERMINE THE LONG-TERM MECHANICAL PROPERTIES OF METALS SUBJECTED TO MECHANICAL STRESS AT ELEVATED TEMPERATURES AND NEUTRON IRRADIATION - Final Report by W. SIEGFRIED and S. ZIMERING (Battelle Memorial Institute)

European Atomic Energy Community - EURATOM
EURATOM/US Agreement for Cooperation
EURAEC Report No. 1921 prepared by the Battelle Memorial Institute, Geneva (Switzerland)
Euratom Contracts No. 100-62-12 RDS and No. 057-64-7 TEES
Brussels, April 1968 - 68 Pages - 26 Figures - FB 100

Improvement of the determination of long-time mechanical properties of metals stressed at high temperature under irradiation is studied by means of solid state physics.

The following problems had to be solved :

- a) Describing the time-to-rupture curves and the curves stress-creep rate mathematically by means of a uniform mathematical function.
- b) Deviding the rupture process in the time-to-rupture test into : mechanisms of deformation, separation, constriction and structural effects.
- c) Calculating the physical values on the basis of physical elementary mechanisms.

Results :

1. A uniform mathematical determination of results has been possible by applying the exponential function of real order to time-to-rupture tests.
2. Applying some valid simplifications, the following values can be calculated on the basis of results of time-to-rupture tests with indication of rupture elongation :
 - 2.1. Number of fissure germs as a function of secondary creep rate.
 - 2.2. Secondary creep rate as a function of stress.
 - 2.3. Volume of activation as a function of stress.
3. Dependence of temperature of these values gives indications on stress changes during time-to-rupture test.
4. Time-to-rupture tests have been made with and without irradiation.

The following problems had to be solved :

- a) Describing the time-to-rupture curves and the curves stress-creep rate mathematically by means of a uniform mathematical function.
- b) Deviding the rupture process in the time-to-rupture test into : mechanisms of deformation, separation, constriction and structural effects.
- c) Calculating the physical values on the basis of physical elementary mechanisms.

Results :

1. A uniform mathematical determination of results has been possible by applying the exponential function of real order to time-to-rupture tests.
2. Applying some valid simplifications, the following values can be calculated on the basis of results of time-to-rupture tests with indication of rupture elongation :
 - 2.1. Number of fissure germs as a function of secondary creep rate.
 - 2.2. Secondary creep rate as a function of stress.
 - 2.3. Volume of activation as a function of stress.
3. Dependence of temperature of these values gives indications on stress changes during time-to-rupture test.
4. Time-to-rupture tests have been made with and without irradiation.

EUR 3752 e

EUROPEAN ATOMIC ENERGY COMMUNITY - EURATOM

**RESEARCH TO DETERMINE THE LONG-TERM MECHANICAL
PROPERTIES OF METALS SUBJECTED TO MECHANICAL STRESS
AT ELEVATED TEMPERATURES AND NEUTRON IRRADIATION**

Final Report

by

**W. SIEGFRIED and S. ZIMERING
(Battelle Memorial Institute)**

1968



**EURATOM/US Agreement for Cooperation
EURAEK Report No. 1921 prepared by the
Battelle Memorial Institute, Geneva - Switzerland**

**Euratom Contracts No. 100-62-12 RDS
and No. 057-64-7 TEES**

SUMMARY

Improvement of the determination of long-time mechanical properties of metals stressed at high temperature under irradiation is studied by means of solid state physics. The following problems had to be solved :

- a) Describing the time-to-rupture curves and the curves stress-creep rate mathematically by means of a uniform mathematical function.
- b) Deviding the rupture process in the time-to-rupture test into : mechanisms of deformation, separation, constriction and structural effects.
- c) Calculating the physical values on the basis of physical elementary mechanisms.

Results :

1. A uniform mathematical determination of results has been possible by applying the exponential function of real order to time-to-rupture tests.
2. Applying some valid simplifications, the following values can be calculated on the basis of results of time-to-rupture tests with indication of rupture elongation :
 - 2.1. Number of fissure germs as a function of secondary creep rate.
 - 2.2. Secondary creep rate as a function of stress.
 - 2.3. Volume of activation as a function of stress.
3. Dependence of temperature of these values gives indications on stress changes during time-to-rupture test.
4. Time-to-rupture tests have been made with and without irradiation.

KEYWORDS

MECHANICAL PROPERTIES
MATHEMATICS
RUPTURE
STRESSES
HIGH TEMPERATURE
NEUTRON BEAMS
METALS

CREEP
MECHANICAL STRUCTURES
DEFORMATION
COTTRELL THEORY
TENSILE PROPERTIES
CRACKS

TABLE OF CONTENTS

	Page
SUMMARY	
1. STATEMENT OF THE PROBLEM	1
2. FUNDAMENTAL CONSIDERATIONS	1
2.1. Extrapolation procedures used for time-to-rupture tests	1
2.2. Principle for solving the problem	3
2.2.1. Introduction of a new function for the mathematical representation of the creep process and time-to-rupture curves	3
2.2.1.1. Extrapolation by an Exponential Function of Real Order	4
2.2.2. Establishment of a quantitative relationship between time-to-rupture tests and physical investigations	9
2.2.2.1. General situation	9
2.2.2.2.1. Mechanisms of deformation	10
2.2.2.2.2. Mechanisms of separation	10
2.2.2.2.3. Geometrical instability	10
2.2.2.3. Determining the relationship between the elementary mechanisms and the results of time-to-rupture tests	11
3. PROCEDURE OF INVESTIGATION	12
3.1. General remarks	12
3.1.1. Subdivision of the different mechanisms into classes	12
3.1.1.1. Mechanisms of deformation	13
3.1.1.2. Mechanisms of formation of rupture	13
3.1.1.3. Changes in material during a long period of time	13
3.1.2. Interaction of the various mechanisms	13
3.1.3. Simplifications introduced	14
3.2. Procedure of calculations	15
3.2.1. Determining the shape of the time-to-rupture curve on the basis of the relationship between stress and creep rate	15
3.2.2. Determining the creep law on the basis of the shape of the time-to-rupture curve	17
3.2.3. Determining the formation of fissures	18
3.2.4. Calculation of values with physical significance	21

	Page
4. DETAILED CALCULATION OF SPECIAL EXAMPLES	21
4.1. Approximations for the time-to-rupture curve	21
4.2. Discussion of examples	23
4.2.1.1. Results of alloy 1	24
4.2.1.2. Results of alloy 2	24
4.2.2. Stainless steel 304	24
4.2.3. Cr-Mo-V cast steel	26
4.3. Separation of mechanisms of deformation and formation of fissures from those of long-time structural changes	27
4.3.1. Development of working assumptions	28
5. CONCLUSIONS	33
 PUBLICATIONS DURING 1965	 34
PUBLICATIONS DURING 1966	35
REFERENCES	36

SUMMARY

The possibilities of improving the determination of long-time mechanical properties of metals being subjected to mechanical stress at elevated temperature, and under the effect of neutron irradiation, are investigated in more detail. An essential improvement is possible if one succeeds in applying the results of investigations made in Solid-State Physics in a quantitative way to determining the time-to-rupture strength of metals.

This presupposes, however, the solution of the following sub-problems :

- a) Describing the time-to-rupture curves and the curves stress-creep rate mathematically by means of a uniform mathematical function.
- b) Dividing the rupture process in the time-to-rupture test into the following classes of partial mechanisms :
 - (b₁) Mechanisms of deformation
 - (b₂) Mechanisms of separation
 - (b₃) Formation of a constriction
 - (b₄) Structural changes of the material.
- c) Calculating the physical values which can be determined, too, on the basis of the known physical elementary mechanisms.

The given assignment has been fulfilled on the following basis :

1. A uniform mathematical determination of results has been possible by applying the exponential function of real order, discovered only a few years ago, to time-to-rupture tests.
2. On application of certain simplifications whose field of validity, however, has been carefully tested, the following values can be calculated on the basis of results of time-to-rupture tests with indication of rupture elongation :

- 2.1. Number of fissure germs as a function of secondary creep rate.
 - 2.2. Secondary creep rate as a function of stress .
 - 2.3. Volume of activation as a function of stress.
3. It is possible to obtain indications on structural changes during the time-to-rupture test by investigating the dependence of temperature of these values.
4. Different series of time-to-rupture tests with and without neutron irradiation have been investigated.

**RESEARCH TO DETERMINE THE LONG-TERM MECHANICAL
PROPERTIES OF METALS SUBJECTED TO MECHANICAL STRESS
AT ELEVATED TEMPERATURES AND NEUTRON IRRADIATION (*)**

1. STATEMENT OF THE PROBLEM

To develop extrapolation methods for determining the influence of neutron irradiation on high temperature-creep properties of metals for the construction of nuclear reactors.

2. FUNDAMENTAL CONSIDERATIONS

2.1. Extrapolation procedures used for time-to-rupture tests

2.1.1. The following simplifications have been introduced for these extrapolation procedures :

(*) Manuscript received on February 1, 1968.

- a) Time to rupture is inversely proportional to the secondary creep rate.
- b) It is assumed that the creep process is a so-called "rate-process" for which the following equation is valid :

$$\dot{\epsilon} = A e^{-\Delta H/RT} \quad (1)$$

A = function of σ

ΔH = heat of activation = function of σ and T

- c) Furthermore, it is assumed that the isothermal time-to-rupture curves being plotted at different temperatures can be converted into one another by a mere translation and rotation of one single curve.

2.1.2. Despite the fact that these procedures without neutron irradiation partially yield quite good results, they still show a number of shortcomings. In general, it can be said that their accuracy for practical requirements is insufficient. The causes of these shortcomings are the following :

- a) The scattering of results of time-to-rupture tests generally is very great, and the number of test results available is relatively small in consequence of high apparatus expenditure. It has not yet been possible to solve the problem of scattering of test results in a satisfactory way.
- b) The simplifications introduced are excessive in many cases. The assumption of a constant elongation of rupture is no longer admissible, especially insofar as embrittlement processes take place.

- c) Physical investigations in this field show that very many elementary mechanisms can be active. Their interaction is so multiform that a purely phenomenological kind of consideration, without going into the details of the physical processes, cannot be successful.

Therefore, a method of solving the entire problem of extrapolating time-to-rupture tests with and without neutron irradiation, on the basis of a much better consideration of results of physical investigations, has been sought.

2.2. Principle for solving the problem

To improve on the situation, the solution of the following problems is necessary :

- a) Introducing mathematical functions for the description of the time-to-rupture curves and the stress dependence of the creep rate. The existence of such functions is a presupposition for dealing with the problem of scattering in an objective way.
- b) Establishing a quantitative relationship between the results of time-to-rupture tests and the physical investigations.

2.2.1. Introduction of a new function for the mathematical representation of the creep process and time-to-rupture curves

2.2.1.1. Extrapolation by an Exponential Function of Real Order

By an analysis of the experimental results and by theoretical consideration, it has been found (see [1, p. 26 and pp. 55-86]) that a general representation of $\dot{\epsilon}$ as function of σ is given by the exponential function of real order - $\varrho_r(\sigma)$ containing three parameters of the temperature : the order r_T , and the two multipliers C_T and a_T of σ and $\dot{\epsilon}$, i.e.,

$$\dot{\epsilon} \approx \frac{\varrho_{r_T}(C_T \sigma)}{a_T} \quad (2)$$

The representation (2) makes it possible

- I) to determine for every temperature a middle curve giving $\dot{\epsilon}$ as function of σ ;
- II) to evaluate better a very long time-to-rupture $t_B = 1/\dot{\epsilon}$;
- III) to estimate the order r_T of the exponential function for a low temperature by the values and the variation of the values of r_T for some higher temperatures, and
- IV) to study the physical processes which take place during creep of industrial steels by the change of r_T with the temperature and at constant temperature with the stress.

The definition and the numerical evaluation of $\varrho_r(\sigma)$ is made by an auxiliary function $A(\sigma)$, which is defined by the following functional equation :

$$\left. \begin{aligned}
 A(e^\sigma - 1) &= A(\sigma) + 1 ; & A(1) &= 0, \\
 \text{and } A'(\sigma) &\text{ is totally monotonic for every } \sigma > 0
 \end{aligned} \right\} \quad (3)$$

G. Szekeres [2] has proved that (3) defines a unique function $A(\sigma)$, and has established a table of $A(\sigma)$ ([2, pp. 326-329]) which has been completed by us ([1, pp. 106-114]).

Defining the exponential function of the entire order $e_n(\sigma)$ by

$$e_n(\sigma) = \overset{\text{n times}}{e^{e^{\dots^{e^\sigma - 1}} - 1}} - 1, \quad n = 1, 2, \dots$$

we obtain by (3),

$$A[e_n(\sigma)] - A(\sigma) = n, \quad n = 1, 2, \dots,$$

i.e.,

$$e_n(\sigma) \equiv A^{-1}[A(\sigma) + n]; \quad (4)$$

where $A^{-1}(\sigma)$ is the reciprocal function of $A(\sigma)$:

$$A^{-1}[A(\sigma)] = \sigma.$$

The property (4) permits the exponential function of real order r to be defined by

$$e_r(\sigma) \equiv A^{-1} [A(\sigma) + r].$$

(The curve of $e_r(\sigma)$ with logarithmic scale is given in Fig. 1.) It has been proved ([1, p. 16]) that a function $f(\sigma)$ can be described by an exponential function of real order, i. e.,

$$f(\sigma) \approx \frac{e_r(C\sigma)}{a},$$

where a , C and r are constants, if and only if

$$\Delta(\sigma) \stackrel{\text{def}}{=} A[f(\sigma)] - A(\sigma)$$

is a monotonic bounded sequence. This last condition is satisfied by every alloy that has been examined by us (see the list of alloys in [3, table 1]).

A method has been developed for the determination of the parameters a_T , C_T and r_T (see [1, p. 20]), which enables the corresponding equation (2) to be found by some numerical values of $(\sigma; \dot{\epsilon})$ of short time of rupture (an example is given in TABLE I below and Fig. 2). The equation (2) permits $t_B = 1/\dot{\epsilon}$ to be evaluated for a long time of rupture. For an illustration, the evaluation of a very long time of rupture for X21 Cr-Mo-V121 steel (0.19 C; 13.28 Cr; 1.19 Mo; 0.30 W; 0.34 V) at 550°C is indicated.

TABLE 1

AN EXAMPLE OF THE CORRESPONDING EQUATIONS (2)
FOR A CARBON-STEEL
(0.09 C normalized at 920°C)

Temperature °C	Equation
525	$\dot{\epsilon} \approx \frac{e^{0.897 (1.279214 \sigma)}}{2.340094}$
500	$\dot{\epsilon} \approx \frac{e^{0.961 (0.971555 \sigma)}}{5.255438}$
475	$\dot{\epsilon} \approx \frac{e^{0.953 (0.885610 \sigma)}}{11.133235}$
450	$\dot{\epsilon} \approx \frac{e^{1.079 (0.575646 \sigma)}}{19.79454}$
435	$\dot{\epsilon} \approx \frac{e^{1.096 (0.541785 \sigma)}}{64.42444}$
425	$\dot{\epsilon} \approx \frac{e^{1.145 (0.442805 \sigma)}}{40.3161}$

First it can be seen that the formula (2) gives a good approximation for a higher temperature (600°C) which shows that the dispersion is not too large; and then, by a few numerical results of short time of rupture (till 4500 h), the values of the parameters at 550°C are determined. It is found that

$$C_T = 0,165 ; \quad a_T = 5 \quad \text{and} \quad r_T = 1,305 ;$$

i. e.

$$\dot{\epsilon} \approx \frac{e_{1,305}(0,165\sigma)}{5} = \frac{A^{-1} \{ A(0,165\sigma) + 1,305 \}}{5} \quad (5)$$

By the equation (5), the value of $t_B = 1/\dot{\epsilon}$ is found, using $A(\sigma)$ 'S table. For example, for $\sigma = 17,5 \text{ kg/mm}^2$

$$\dot{\epsilon} = \frac{\{A^{-1} A(0,165 \cdot 17,5) + 1,305\}}{5} = 12,163 \cdot 10^{-6}/\text{h} ,$$

which gives

$$t_B = \frac{1}{\dot{\epsilon}} = 82.215 \text{ h.}$$

(The interrupted experimental result is 80 000 h. - see some details in [1, p. 43]). The error in $\dot{\epsilon}$ depends on the precision of the value of r_T . For example, a precision of 0,01 in r_T gives the value of $\dot{\epsilon}$ with an accuracy of 5 % for $\dot{\epsilon} \leq 50$ (see [1, p. 45]).

2.2.1.2. If a function is available to determine the slope of the time-to-rupture curves mathematically in the whole field of stress, then a new basis presents itself for the problem of scattering. A rational method has been developed which permits the parameters of the mean value curve to be determined in an objective way by means of a given amount of points measured.

2.2.2. Establishment of a quantitative relationship between time-to-rupture tests and physical investigations.

2.2.2.1. General situation

The major difficulty which has to be overcome when trying to solve this sub-problem lies in the fact that a large number of elementary mechanisms can be active. These elementary mechanisms are not yet completely investigated, and the laws governing their interaction are still fairly vague. For this reason it seems to be too early to determine the quantitative relationship between the results of time-to-rupture tests and the physical investigations at this stage. A more accurate analysis showed, however, that the various elementary mechanisms concerned can be divided into different classes according to their kinematic behaviour, and that a division of the rupture process into the different classes of mechanism is possible without knowing all details of the elementary mechanisms.

2.2.2.2. According to the kinematic behaviour, the mechanisms can be classified as follows :

2.2.2.2.1. Mechanisms of deformation

First and foremost, these are the different mechanisms of movement of dislocations which, as a rule, bring about only a deviation of the material.

2.2.2.2.2. Mechanisms of separation

These are mechanisms by means of which a separation of the material takes place. In principle, these mechanisms again can be combined in two groups, i. e. :

- a) Formation of fissure germs and growth of the same (Cottrell's mechanism).
- b) Instability of fissures according to the model originally described by Griffith.

2.2.2.2.3. Geometrical instability

In this case, the formation of a constriction is concerned, whereby, at any point of the test bar, a local deformation takes place. By means of this local deformation the effective stress increases, causing an additional local deformation and, finally, rupture by formation of a constriction at this point. For this process of formation of rupture, two different mechanisms have in principle to be distinguished, viz :

- a) Plastic body.

In this material, there exists a relationship between stress and deformation. The formation of a constriction in such a material is possible only once the external stress has exceeded a certain limiting value, i. e. the maximum stress.

b) Quasi-viscous material.

For such a material, a mathematical relationship exists between stress and rate of deformation. The formation of a constriction takes place at any small external stress, and only the rate of formation of a constriction is altered by the amount of external stress.

2.2.2.3. Determining the relationship between the elementary mechanisms and the results of time-to-rupture tests

The first investigations for determining the relationship between the results of time-to-rupture tests and the elementary creep mechanisms have been made by Sherby and Dorn, specifically on pure aluminium. It has been found in the course of these investigations that for pure aluminium, a formula according to equation (1) is valid for the secondary creep rate. In this case, A is only a function of stress, whereas ΔH can be regarded as constant in certain temperature ranges.

Our work began with a continuation of formulas laid down by Sherby and Dorn, in that an endeavour was made for various technical steels and alloys to determine the value A in equation (1) as a function of stress, and the heat of activation ΔH as a function of temperature. Such a determination proved possible, but is not sufficiently accurate for practical application to an extrapolation after long times. Also, it has not been possible to explain the dependence of the value A on stress and that of ΔH on temperature by means of the known mechanisms of dislocation, as has been the case for pure aluminium. It has been found that a decrease of the apparent energy of activation at elevated temperatures occurs in alloys with precipitation effects. This decrease is quite difficult to explain by means of the models established by the theory of dislocation. However, as our investigations have shown, it can be explained by an overageing of precipitations

taking place, in general, at high temperatures and long test times.

Considering the fact that the laws which determine the precipitations, and their interaction with the creep processes, are extremely complex, it is out of question that an appropriate extrapolation method under the presence of neutron irradiation can be derived on the basis of purely phenomenological generalizations. It therefore proved necessary to further develop the theories established by Sherby and Dorn, in that the rupture process in the time-to-rupture test has been subdivided into the following classes of process :

- a) Processes of deformation
- b) Processes of separation
- c) Formation of geometrical instability
- d) Processes of material changes during the creep test (annealing - and precipitations-processes)

3. PROCEDURE OF INVESTIGATION

3.1. General remarks

3.1.1. Subdivision of the different mechanisms into classes

The single mechanisms can be subdivided into the following classes :

3.1.1.1. Mechanisms of deformation

- a) Monocrystal
- b) Polycrystal (interaction of crystallite and grain boundary).

3.1.1.2. Mechanisms of formation of rupture

- a) Growth of fissures in the grain boundaries
- b) Instability of fissures
- c) Geometrical instability.

3.1.1.3. Changes in material during a long period of time

3.1.2. Interaction of the various mechanisms

These various classes of mechanism influence one another mutually. Fig. 3 gives a schematic representation of relationships. The interaction can be summarized as follows : first, a deformation of material takes place, namely by deformation of crystals on the one hand and by processes of deformation in the grain boundaries on the other. This deformation causes two new phenomena to come into play, i. e. :

3.1.2.1. Geometrical elongation of the specimen and formation of a constriction. The form of the constriction is determined by the relationship between stress and creep rate. A rise of the effective stress occurs in consequence of the formation of a constriction.

3.1.2.2. Development of fissure germs according to various processes and growth of these via stress-directed diffusion processes.

3.1.2.3. Rupture of specimen when stress increase as a result of formation of a constriction is high enough to induce the instability of fissures.

3.1.3. Simplifications introduced

The scheme in Fig. 4 graphically shows the simplifications which have been taken as a basis for our calculations. These can be summarized as follows :

3.1.3.1. Time to rupture is so long that the 1st and the 3rd stages of the creep process can be neglected as against the 2nd one.

3.1.3.2. It is assumed that the occurrence of instability of fissures practically coincides with the point of time at which the single fissures meet (Cottrell's criterion).

3.1.3.3. It is supposed that the germination and the growth of fissures can be regarded as two independent processes.

3.1.3.4. It is assumed, further, that the structural changes take place so slowly that mean values may be introduced for the values to be calculated.

3.2. Procedure of calculations

3.2.1. Determining the shape of the time-to-rupture curve on the basis of the relationship between stress and creep rate

The following working assumptions have to be defined mathematically :

a) Presence of a creep law

$$\dot{\epsilon} = \varphi (\sigma)$$

$$\dot{\epsilon} = \text{creep rate} \quad (6)$$

$$\sigma = \text{stress}$$

b) Constancy of volume

$$F \cdot \ell = F_0 \ell_0$$

$$F = \text{cross-sectional area} \quad (7)$$

$$\ell = \text{length}$$

Introducing the physical elongation, we obtain

$$\epsilon = \ell_n \frac{\ell}{\ell_0} = \ell_n \frac{F_0}{F} \quad (8)$$

c) Constancy of load

$$\sigma_0 F_0 = \sigma \cdot F. \quad (9)$$

Combination of equations (6) - (9) yields

$$\frac{d\varepsilon}{dt} = \dot{\varepsilon} = \varphi (\sigma_0 \cdot \exp. \varepsilon) \quad (10)$$

and by integration, the time-to-rupture

$$t = \int_{\varepsilon_0}^{\varepsilon_B} \frac{d\varepsilon}{\varphi(\sigma_0 \exp \varepsilon)} \quad (11)$$

ε_B can be calculated from the reduction of area of broken specimens according to equation (12).

$$\varepsilon_B = - \ln \left(1 - \frac{\Psi_B}{100} \right) \quad (12)$$

Ψ_B = reduction of area in %

Introducing the substitution $\sigma_0 \cdot \exp \varepsilon = z$, we obtain equation (13).

$$t = \int_{\sigma_0 \exp. \varepsilon_0}^{\sigma_0 \exp. \varepsilon} \frac{dz}{z \cdot \varphi(z)} \quad (13)$$

3.2.2. Determining the creep law on the basis of the shape of the time-to-rupture curve

Once the shape of the time-to-rupture curve is available, the relationship between stress and creep rate can be derived in a simple way. For that purpose, we need the nominal stress (Fig. 5), the slope of the tangent line to the time-to-rupture curve, and the elongation of rupture as a function of time-to-rupture. By differentiation of equation (13), we obtain equation (14) :

$$\frac{1}{m} = \frac{1}{t_B} \left\{ \frac{1}{[\varphi(\sigma)] \sigma_o \exp \varepsilon_o} - \frac{1}{[\varphi(\sigma)] \sigma_o \exp \varepsilon_B} \right\} \quad (14)$$

$$m = - \frac{d \log \sigma_o}{d \log t_B}$$

Equation (14) is valid for any integrable function of $\varphi(\sigma)$. For our calculations, we restrict ourselves to the following types of function, i. e.

a) Hyperbolic creep law

$$v = v_o \sinh \left(\frac{\sigma}{\sigma_1} \right) = \varphi(\sigma) \quad (15)$$

b) Exponential function

$$v = A \sigma^n = \varphi(\sigma) \quad (16)$$

c) Hyperbolic creep law with parameters depending on stress

$$v = v_0(\sigma) \sinh \frac{\sigma}{\sigma_1(\sigma)} = \varphi(\sigma) \quad (17)$$

It could be shown that equation (17) is admissible under certain restrictive conditions. These conditions, however, are satisfied mostly for time-to-rupture curves plotted in practice.

3.2.3. Determining the formation of fissures

The number of fissure germs is calculated on the basis of calculations introduced by Cottrell⁴⁾, consisting mainly in the fact that the process of germination and the growth of fissures are supposed to be two physically different and independent processes. In the calculation, this fact is expressed by introduction of a fictive germ number as calculating value at a time $t = 0$. Cottrell's equation can now be improved by introducing into the calculation the increase in stress owing to the formation of a constriction and that as a result of a decrease in the supporting cross-section because of the growth of fissures.

Cottrell's equation for the growth of fissures by stress-directed diffusion of atoms and holes reads as follows :

$$\frac{dr}{dt} = \frac{3 \Omega \delta D \sigma}{a r k T} \quad (18)$$

r = radius of fissure

Ω = volume of an atom (or hole)

δ = thickness of grain boundary

D = diffusion constant

a = mean distance of fissure germs

σ = stress

Into this equation we have to introduce the increase in stress by formation of a constriction and that by decrease of supporting cross-section as a result of the growth of fissures (see equations (19) and (20) :

$$\sigma_1 = \sigma_0 \exp(\epsilon) \quad (19)$$

$$\sigma = \frac{\sigma_1}{1 - \frac{4}{3} \pi \frac{r^3}{a^3}} \quad (20)$$

Combining equations (18) - (20), we obtain equation (21)

$$r \cdot \frac{dr}{dt} = \frac{3 \Omega D \sigma \delta}{a k T} \frac{a^3 \exp(\epsilon)}{a^3 - \frac{4}{3} \pi r^3} \sigma_0 \quad (21)$$

From equation (10), there follows that

$$dt = \frac{d\epsilon}{\varphi(\sigma_0 \exp \epsilon)} \quad (22)$$

By substituting (22) in (21) , it is possible to integrate this equation. The result is represented in equations (23) to (26). It is impossible to determine all values appearing in equation (23). Calculation gives only a combination of different values, i. e. the value indicated in equation (23).

$$p = \frac{a^3 k T}{Q D \delta} \quad (23)$$

Introducing the value

$$\chi = \frac{1}{\sigma_0} \int_{\sigma_0}^{\sigma_0 \exp \epsilon_B} \frac{du}{\varphi(u)} \quad (24)$$

we obtain equation (25)

$$p = 25.8 \cdot \chi \cdot \sigma_0 \quad (25)$$

The value χ is of the dimension of time and, as practical calculations show, differs only little from the time-to-rupture. It is therefore possible to introduce a value $\alpha = \frac{\chi}{t_B}$ which is only slightly different from 1. Finally, we obtain

$$p = \alpha \cdot 25.8 t_B \sigma_0 \quad (26)$$

The most important result obtained was that the constriction of rupture had but little influence on the calculated number of fissure germs.

3.2.4. Calculation of values with physical significance

For characterizing the creep process, the following values are of importance :

- a) Number of fissure germs at a time $t = 0$

$$\frac{p}{\alpha} = \frac{a^3 k T}{\Omega D \delta \alpha} = 25.8 t_B \cdot \sigma_o \quad (27)$$

- b) Volume of activation

$$v^* = kT \frac{d \ln v_{\text{sec}}}{d \sigma} \quad (28)$$

- c) Secondary creep rate

$$v_{\text{sec}} = \varphi(\sigma) \quad (29)$$

4. DETAILED CALCULATION OF SPECIAL EXAMPLES

4.1. Approximations for the time-to-rupture curve

For the examples to be discussed, the time-to-rupture curve is assembled piece by piece by means of linear functions. The mathematical

definition of a straight-line relationship in double logarithmic scale is given by equation (30)

$$\log \sigma_o = \log \sigma_{oo} - \frac{1}{n} [\log t_B - \log t_{Bo}] \quad (30)$$

σ_{oo} and t_{Bo} are any correlated pair of values.

According to equations (31) - (33), the value p , the volume of activation, and the secondary creep rate can be calculated from equation (30).

$$\frac{p}{\alpha} = \left(\frac{\sigma_{oo}}{t_{Bo}} \right)^n \frac{1}{\sigma_o^{n-1}} \quad (31)$$

$$\frac{v^*}{kT} = \frac{n}{\sigma_o} \quad (32)$$

$$v_{sec} = \frac{\text{const}}{t_{Eo}} \left(\frac{\sigma_o}{\sigma_{oo}} \right)^n \quad (33)$$

4.2. Discussion of examples

4.2.1. Analysis of time-to-rupture tests on Cr-Ni-alloys before and after neutron irradiation. These are alloys of Russian origin⁵⁾, as is indicated in Table 2.

TABLE 2

ALLOY	C %	Si	Mn	Cr	Ni	Ti	Al	Fe	B	Zr
XH77T LOP	< 0.06	< 0.6	< 0.40	19-22	Base	2.30- 2.70	0.55- 0.95	≤ 0.4	≤ 0.01	< 0.01
IXI8H9T	0.12	0.80	1.00- 2.00	17-19	9-11	0.50 0.70	-	Base	-	W

4.2.1.1. Results of alloy 1

The result of time-to-rupture tests at 800°C before and after irradiation are plotted in double logarithmic scale in Fig. 6. A strong decrease in stress caused by irradiation has been determined for same times to rupture.

Fig. 7 shows the values for the formation of fissure germs before and after irradiation. It is ascertained that, owing to irradiation, the density of fissure germs has increased approx. fivefold. Since no values of rupture elongation have been indicated for these alloys, the volume of activation and the secondary creep rate could not be calculated.

4.2.1.2. Results of alloy 2

Fig. 8 shows the time-to-rupture tests at 600°C and 700°C before and after neutron irradiation. The corresponding values for fissure germs are represented in Fig. 9. As can be seen, the change of fissure germs in this alloy as a result of irradiation is much smaller than was the case for the preceding alloy. This can be traced back to the fact that the first alloy showed a boron content of approx. 0.01 %, whereas the second showed none. It has been observed metallographically by the authors that actually in the first alloy, formation of fissures takes place by generation of gas in consequence of the boron decomposition during neutron irradiation.

4.2.2. Stainless steel 304⁶⁾

The curves corresponding to in-pile time-to-rupture tests on stainless steel 304 and off-reactor control tests are represented in Fig. 10. To obtain a comparison with the Russian results, the value p as a function

Time to rupture has been plotted in Fig. 11. Here it can be seen that, under the influence of neutron irradiation, the number of fissure germs is somewhat increased, although insignificantly only, at 704° and 760°C, whereas at 816°C it remains practically constant.

In Fig. 12, the secondary creep rate has been plotted as a function of stress. At 704° and 816°C, a decrease of secondary creep rate is determined by irradiation, whereas at 760°C it is not changed by neutron irradiation. The change of secondary creep rate owing to neutron irradiation is the resultant of two opposite influences, i. e. on the one hand the time-to-rupture curve is displaced downwards, which corresponds to an increase in the secondary creep rate at same stress, and on the other hand the elongation decreases which, kinematically, means a decrease of secondary creep rate. The different behaviour at 760°C compared to 704° and 816°C is to be traced back to the fact that at 760°C the displacement of the time-to-rupture curve downwards is larger than at the two remaining temperatures, and elongation of rupture remains unchanged.

Value p as a function of secondary creep rate has been plotted in Fig. 13. This kind of representation has been chosen because all models for the formation of fissures start from the principle that germination of fissures is caused by deformation. Therefore, it is to be expected that this representation includes the physical relationship far better than that for the value p as a function of time to rupture. Fig. 13 shows that actually this is true.

Value v^*/kT , i. e. the volume of activation, has been plotted in Fig. 14 in dependence of time to rupture. As can be seen, the volume of activation is reduced in a creep process under neutron irradiation.

4.2.3. Cr-Mo-V cast steel⁷⁾

This example was chosen because the time-to-rupture curve shows certain anomalies which have been determined experimentally. Fig. 15 shows a time-to-rupture curve for this cast steel at 500°C, according to the results of a test series conducted at Georg Fischer. As can be seen from this, an unsteady reduction of time to rupture is observed at a certain stress. It seemed to be especially interesting to determine the results of the above-mentioned kinematic analysis of this time-to-rupture curve. The shape of the curve has been approached by the three straight lines plotted in Fig. 15. The secondary creep rate as a function of stress has been plotted in Fig. 16. At the transition of straight line 1 to straight line 2, an unsteady rise of the same occurs.

Fig. 17 shows the value p/α as a function of stress. It can be seen that at the transition of straight line 1 to straight line 2, an unsteady increase in the number of fissure germs is observed which, however, decreases at the transition of 2 to 3.

Very interesting conclusions can be drawn from plotting the value p/α as a function of the secondary creep rate (Fig. 18). As can be seen, the curves for the straight lines 1 and 2 nearly coincide, and the slope is the same. Whence, it can be concluded that the creep process according to straight line 1 and straight line 2, the same mechanism for the formation of fissure germs is available, whereas for the creep process according to straight line 3, there exists another relationship between germ number and secondary creep rate, as is represented in Fig. 18. The difference between the two mechanisms of germination could for instance lie in the fact that in the creep process according to straight line 3, creep takes place by deformation of the grain boundary, and therefore the local rate of

elongation is much higher than its mean value. The unsteady increase in the number of fissure germs at the transition of curve 1 to curve 2 can be explained by the fact that the creep rate and, consequently, the formation of fissure germs per unit of time have been increased for the creep process according to curve 2; the mechanism of formation of fissures, however, remained unchanged.

This conception is confirmed by regarding the volume of activation as a function of stress (see Fig. 19). As can be seen here, the volume of activation is approximately the same for the creep process according to curves 1 and 2, whereas it is considerably smaller for that according to curve 3.

On the basis of these reflections, the following general statements can be made about the physical processes based on the anomalies mentioned :

- a) The transition of process 1 to process 2 is caused substantially by a softening of the material without the mechanism of formation of fissures being changed.
- b) At the transition of creep process 1 or 2 to creep process 3, there appears a new creep mechanism with a different volume of activation and another mechanism of formation of fissure germs.

4.3. Separation of mechanisms of deformation and formation of fissures from those of long-time structural changes

4.3.1. Development of working assumptions

The structural changes are distinguished from the mechanisms of deformation and formation of fissures by the fact that the former show an energy of activation that in the first approximation can be compared to the energy of activation for the self-diffusion, whereas the latter show an energy of activation that is given first of all by the chemical potential of structural change. This chemical potential, however, is given by the equilibrium lines in the phase diagram and by the amount of undercooling. If ageing and heat-treatments are modified, this part in the energy of activation will be changed above all. We can therefore draw conclusions on the structural changes from the dependence on temperature of values v_o , σ_1 and \underline{a} determined in section 3.2.3. This is only possible, however, if the general structure of the equations is known by means of which the influence of structural changes on the mechanisms of deformation is determined. To determine this structure, we proceed as follows :

It was possible to give some indications on these ratios for an important special case, namely for precipitation and growth of a secondary phase from solid solution in combination with climbing of screw dislocations across these precipitations. The following equations have been obtained for the values v_o and σ_1 :

$$\log v_o + \frac{\Delta H_1}{2,3 RT} = \varphi_2 \left\{ \frac{\Delta H_3}{2,3 RT} - \log t_B \right\} \quad (34)$$

$$\log \sigma_1 - \frac{\Delta H_4}{2,3 RT} = \varphi_4 \left\{ \frac{\Delta H_5}{2,3 RT} - \log t_B \right\} \quad (35)$$

$\Delta H_1, \Delta H_3, \Delta H_4, \Delta H_5$ = heat of activation

ΔH_1 , and ΔH_4 strongly dependent on the chemical potential

ΔH_3 and ΔH_5 not very different from heat of activation for self-diffusion.

These equations mean that, in case $\log v_o + \frac{\Delta H_1}{2,3 RT}$ is plotted in dependence of $\frac{\Delta H_3}{2,3 RT} - \log t_B$, one single curve for all temperatures is obtained. The energies of activation ΔH_1 and ΔH_3 in this case are functions of temperature.

In the same way, one single curve is also obtained if $\log \sigma_1 - \frac{\Delta H_4}{2,3 RT}$ is plotted in dependence of $\frac{\Delta H_5}{2,3 RT} - \log t_B$.

To check the accuracy of these reflections in greater detail, time-to-rupture tests on a Cr-Mo-V-steel described by W.F. Brown Jr. et al. have been evaluated. Fig. 20 shows the nominal stress, and Fig. 21 the elongation of rupture as a function of time-to-rupture. Using the method described above, the relationship between stress and creep rate has been ascertained from these time-to-rupture tests by determining the values v_o and σ_1 as functions of stress for the equation

$$\dot{\epsilon} = v_o(\sigma) \sinh \left\{ \frac{\sigma}{\sigma_1(\sigma)} \right\}$$

v_o has been plotted in Fig. 22 and σ_1 in Fig. 23 as a function of time to rupture. If equations (34) and (35) are valid, the curves for different temperatures in Figs. 22 and 23 can be brought to coincidence by means of a mere translation.

In Fig. 24, $\frac{\Delta H_1}{2,3 RT} + \log v_o$ has been plotted in dependence of $\frac{\Delta H_3}{2,3 RT} - \log t_B$ for time-to-rupture tests on a Cr-Mo-V-steel. As can be seen, it is possible to draw a single curve through the points obtained. The strong dependence of $\log v_o$ on time to rupture can be explained by the transition of a creep law according to a hyperbolic sine to that according to an exponential function. It is interesting to note that it is possible to find a uniform representation according to equations (34) and (35) for both fields of creep, as well as for the transition of one field of creep to the other. This permits the conclusion on the one hand that the results of theoretical considerations are confirmed by practical tests, and on the other hand that the transition of one field of creep to the other is determined by the growth of precipitations and the processes of overageing.

In Fig. 25, $\log \sigma_1 - \frac{\Delta H_4}{2,3 RT}$ has been plotted in dependence of $\frac{\Delta H_5}{2,3 RT} - \log t_B$. As can be seen, equation (35) can also be confirmed experimentally.

For the energies of activation in dependence of temperature, the following values have been obtained under the assumption that the energy of activation for the self-diffusion is 78 000 cal/mole :

TABLE 3

Temp. °K	ΔH_1	ΔH_3	ΔH_4	ΔH_5
755	73 862	78 000	1 207	79 725
811	76 889	76 000	778	81 250
866	76 418	75 000	554	79 400
923	78 000	78 000	0	78 000

It is now easy to form an idea of the physical meaning of the energies of activation ΔH_1 , ΔH_3 , ΔH_4 , and ΔH_5 , namely as follows :

Creep rate is calculated in dependence of time, i. e. the two values and σ_1 in the case of a two-phase alloy in which ballshaped precipitations develop by means of diffusion processes. The calculation of creep rate based on the model given by Ansell and Weertman for the climbing of new dislocations across precipitations.

For the growth of precipitations, Dorn's approximate calculations have been applied. The changes of coherence stress and surface energy during overageing have not been considered in this approximation. It is furthermore assumed that no formation of new germs for precipitation takes place during the creep process. The free energy for structural changes can be determined from equation (34), as well as from equation (35).

TABLE 4

Temp. °K	ΔU determined from equation (34)	ΔU determined from equation (35)
755	4 162	9 007
811	2 139	4 028
866	- 182	1 954
923	0	0

Calculations gave the values compiled in Table 4 in dependence of temperature. As can be seen, the two values calculated for the energy of activation do not agree closely. However, the differences can be explained easily by means of the simplifications based on the calculation. Mainly, the fact that the precipitations are not ball-shaped but flake-shaped explains, as a single rough calculation shows, the differences observed. Moreover, it is possible that in this alloy formation of germs of precipitations and overageing still take place during the creep process.

These calculations have to be regarded as key test, since very strong simplifications had to be introduced to check the fundamental accuracy of reflections made by means of only a few mathematical calculations. Moreover, the physical investigations concerning the change of precipitations in the course of time and the climbing of dislocations over precipitations have not yet been brought to an end. The results obtained confirm, however, the fundamental accuracy of our concepts. Thus, a basis is obtained for understanding and determining the influence of an annealing treatment on

the long-time mechanical properties at high temperature quantitatively on alloys in which precipitation processes take place.

5. CONCLUSIONS

The described investigations have made it possible to establish in a quantitative way the relationships between the shape of time-to-rupture curves and certain kinematic values which can be calculated on the basis of the physical theories. In this way, a basis is obtained for developing new extrapolation methods by means of which the results of measurements of physical values can be introduced into the calculation quantitatively. It can be expected that, thanks to this fact, a substantial reduction of cost and necessary test time can be achieved for determining the long-time mechanical properties at high temperature and under neutron irradiation.

To check the accuracy of reflections made in the shortest possible time very great simplifications had to be made in several instances in the course of the present investigations. Once the fundamental accuracy of models introduced can be regarded as confirmed, these models can be further developed, and the computing methods applied can be considerably improved.

The results obtained also make it possible to evaluate summarily the available results of technological time-to-rupture tests which have been made at high temperatures and under neutron irradiation, and those of physical investigations as regards the influence of neutron irradiation on the mechanical properties. Considerable improvement of the situation towards determining the long-time mechanical properties and developing new materials can be expected from such an evaluation of investigations already available.

PUBLICATIONS DURING 1965

- 1) W. SIEGFRIED : On the theory of notch-brittleness in steels occurring during time-to-rupture tests.
EURAEK Report No. 1350.
- 2) W. SIEGFRIED : Determination of the elementary mechanisms of the rupture process at creep by evaluation of time-to-rupture tests.
"Symposium sur le comportement à chaud des alliages métalliques", Torino, 29th September, 1965
- 3) W. SIEGFRIED : Nouvelle approche pour l'étude de phénomènes de fragilisation au cours des essais de fluage.
"Journées d'Automne de la Société Française de Métallurgie", Paris, 11th - 15th October, 1965.
- 4) S. ZIMERING : Une nouvelle méthode d'extrapolation du temps de rupture d'un alliage industriel.
Les Mémoires Scientifiques de la Revue de Métallurgie, LXII, No 12, 1965, pp. 939-950.
- 5) W. SIEGFRIED : Untersuchungen über den Zusammenhang zwischen der Form der Zeitbruchlinie warmfester Stähle und den verschiedenen Mechanismen des Kriechvorganges.
Archiv für das Eisenhüttenwesen, Jg. 37, H. 1, 1966, pp. 65-78.
- 6) S. ZIMERING : La fonction exponentielle d'ordre réel et son application pour la description du procédé de fluage. Journal de Mathématiques et de Physique Appliquées (ZAMP), vol. 17, fasc. 3 (1966), pp. 417-424.

PUBLICATIONS DURING 1966

- W. SIEGFRIED and S. ZIMERING : Research to Determine the Long-Term Mechanical Properties of Metals Subjected to Mechanical Stress at Elevated Temperatures and Neutron Irradiation.
EURAE C Report No. 1621.
- S. ZIMERING : Description détaillée d'une méthode d'extrapolation du temps de rupture d'un alliage industriel.
Les Mémoires Scientifiques de la Revue de Métallurgie, LXIII, No 10, Oct. 1966,
pp. 849-862.
- W. SIEGFRIED : Grundsätzliche rheologische und thermodynamische Betrachtungen für die Durchführung von Zeitstandsversuchen unter Neutronenbestrahlung.
[Festigkeitseigenschaften von Baustählen unter Neutronenbestrahlung], Deutsche Rheologische Gesellschaft, Berlin, 8th - 10th June 1966.
-) W. SIEGFRIED : Nouvelles Méthodes pour l'Interprétation Physique des Essais de Durée.
6 èmes Journées des Aciers Spéciaux, Toulouse,
8th - 9th June 1967.

REFERENCES

- 1) S. ZIMERING : A new mathematical function for the general description of the creep process of technical alloys.
USAEC and EURATOM, Contract 100-62-12, First Special Report (March 1964).
- 2) K. W. MORRIS and G. SZEKERES : Tables of the logarithm of iteration of $e^x - 1$.
Australian Math. Journal (1961), pp. 321 - 333.
- 3) W. SIEGFRIED and S. ZIMERING : USAEC and EURATOM, Contract 100-62-12. Fourth Quarterly Report (March 1964).
- 4) A. H. COTTRELL : Intercrystalline creep fractures:
Structural processes in creep, p. 1-18, 1961,
The Iron and Steel Institute, London.
- 5) E. V. GUSEV; P. A. Platonov; N. F. Pravdyuk; N. M. Sklyarov :
Effect of reactor irradiation on stress-rupture strength of austenitic steels and heat-resistant materials based on iron and nickel.
Third United Nations International Conference on the Peaceful Uses of Atomic Energy,
A/Conf. 28/P/339 a.
- 6) N. E. HINKLE: Effect of neutron bombardment on stress rupture properties of some structural alloys.
Symposium on radiation effects on metals and neutron dosimetry.
ASTM Spec. Techn. Publication No 341, pp. 344-358.

- 7) J. JUSCO and K. GUT : Ausscheidungen bei niedrig legiertem,
warmfestem Cr-Mo-V- Stahlguss
während des Zeitstandversuchs.
Schweizer Archiv f. Angewandte Wissenschaft
u. Technik, Jg. 32 (1966), H. 1, p. 16.

Geneva, 16th August 1967
WS/rmd Z 513-8

Fig. 1

The function $er(\delta)$ in logarithmic scale for $r=0; 0,5; 0,75; 1; 1,25; 1,5$ and 2 .

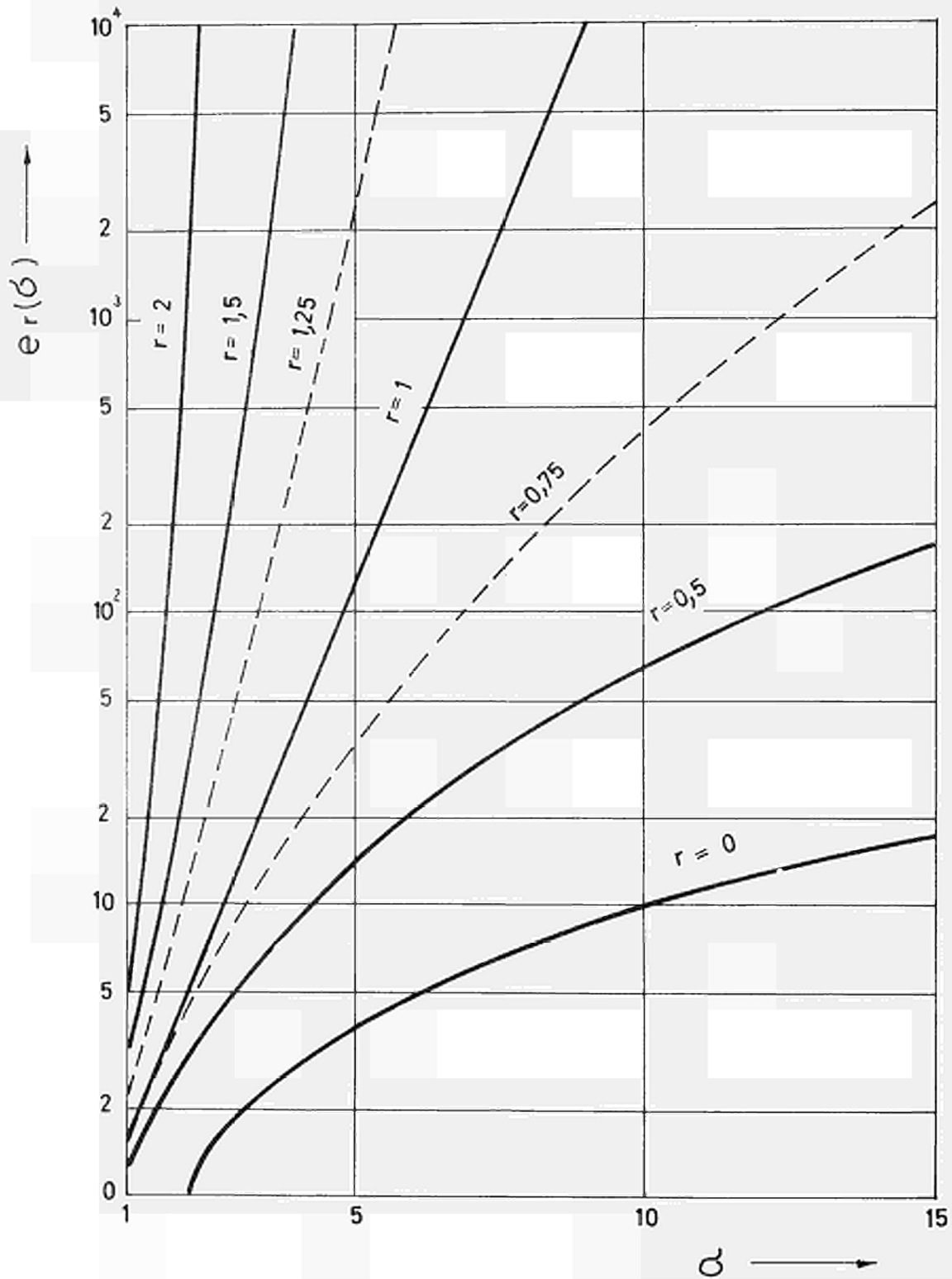


Fig. 2

Representation of $\dot{\epsilon}$ as an exponential function of real order in σ for a carbon steel (0,09 C normalized at 920 °C),

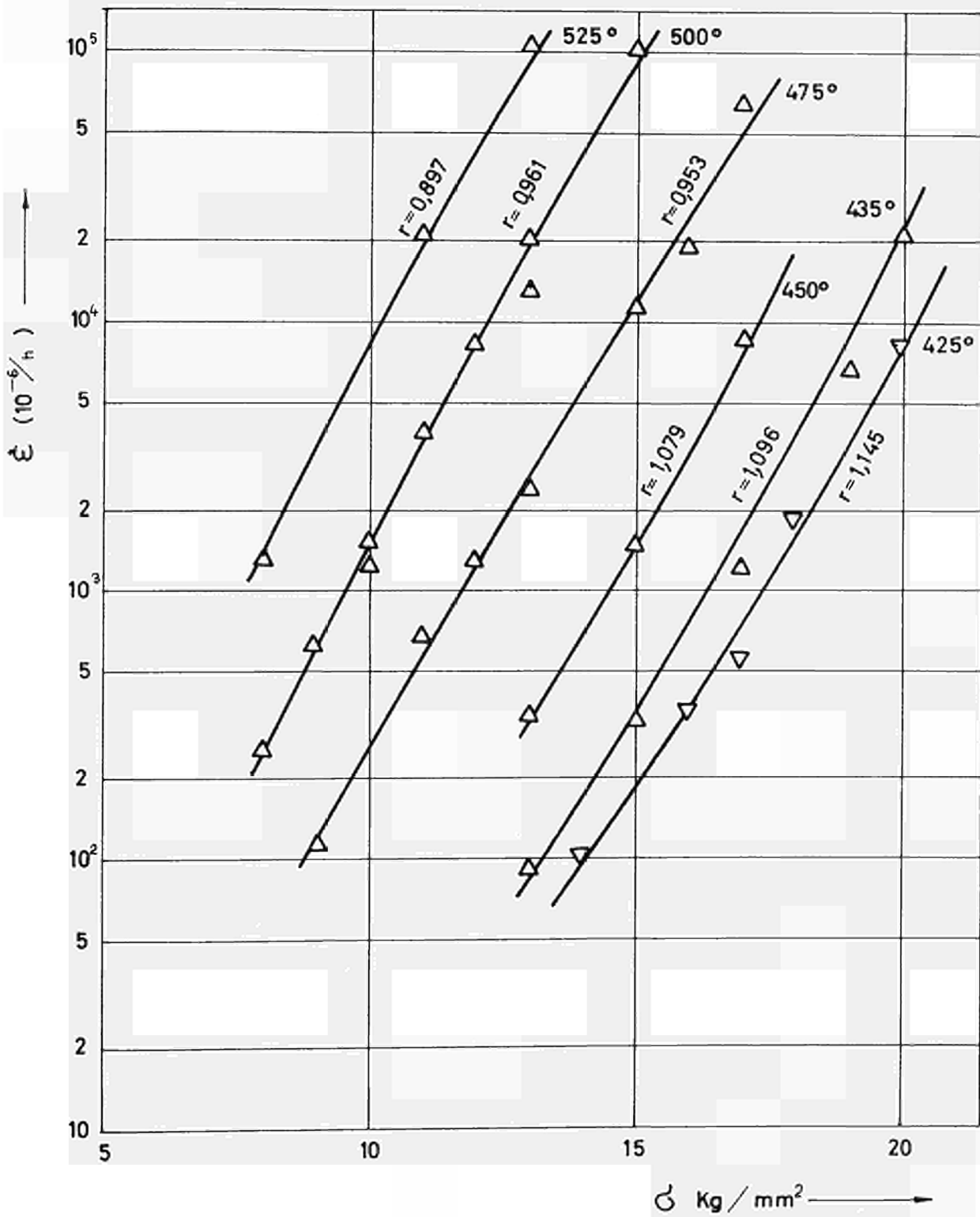
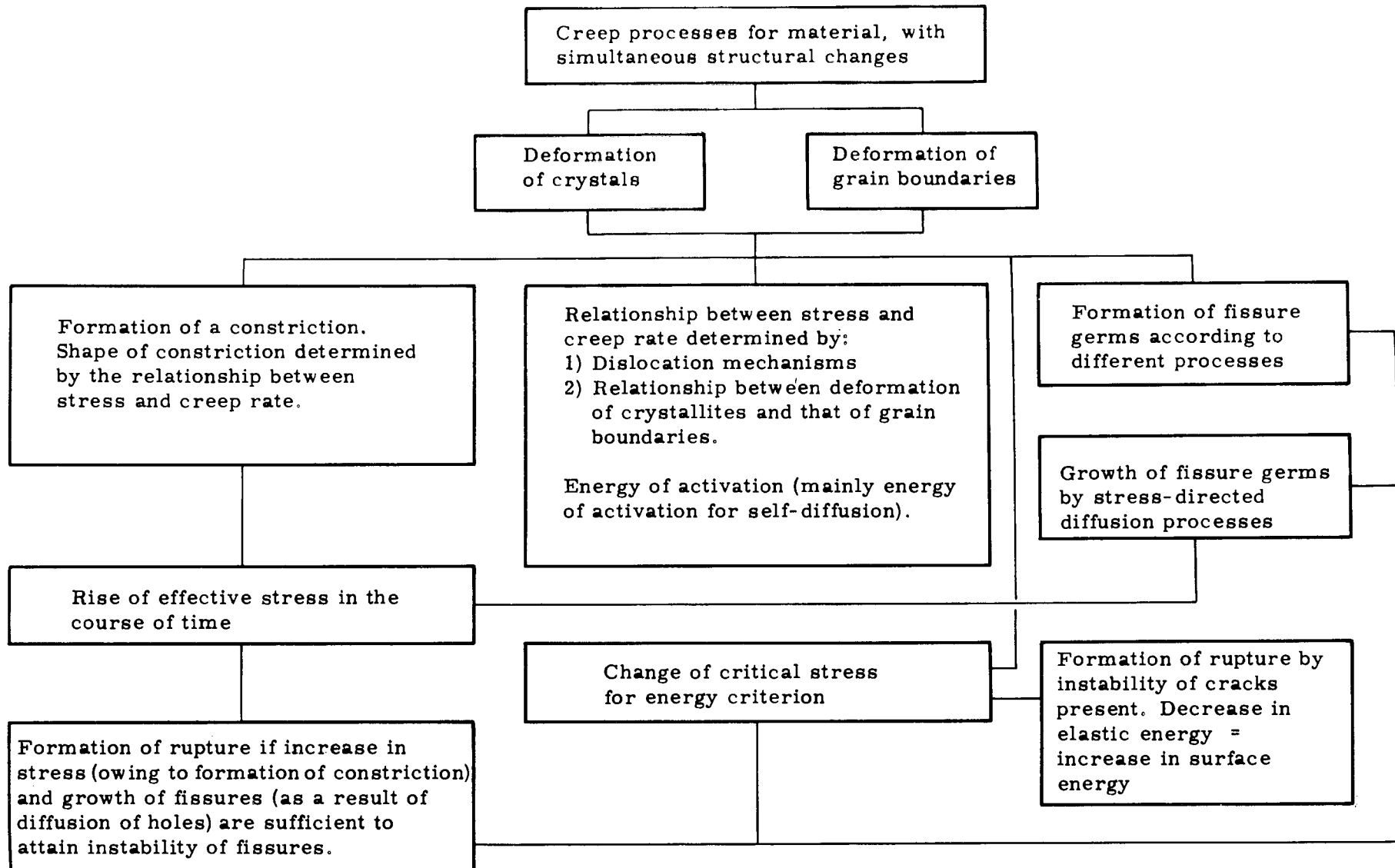


Fig. 3 - Schematic representation of elementary processes taking place during a time-to-rupture test.



SIMPLIFIED SCHEME FOR RUPTURE OF METALS WITHOUT STRUCTURAL CHANGES

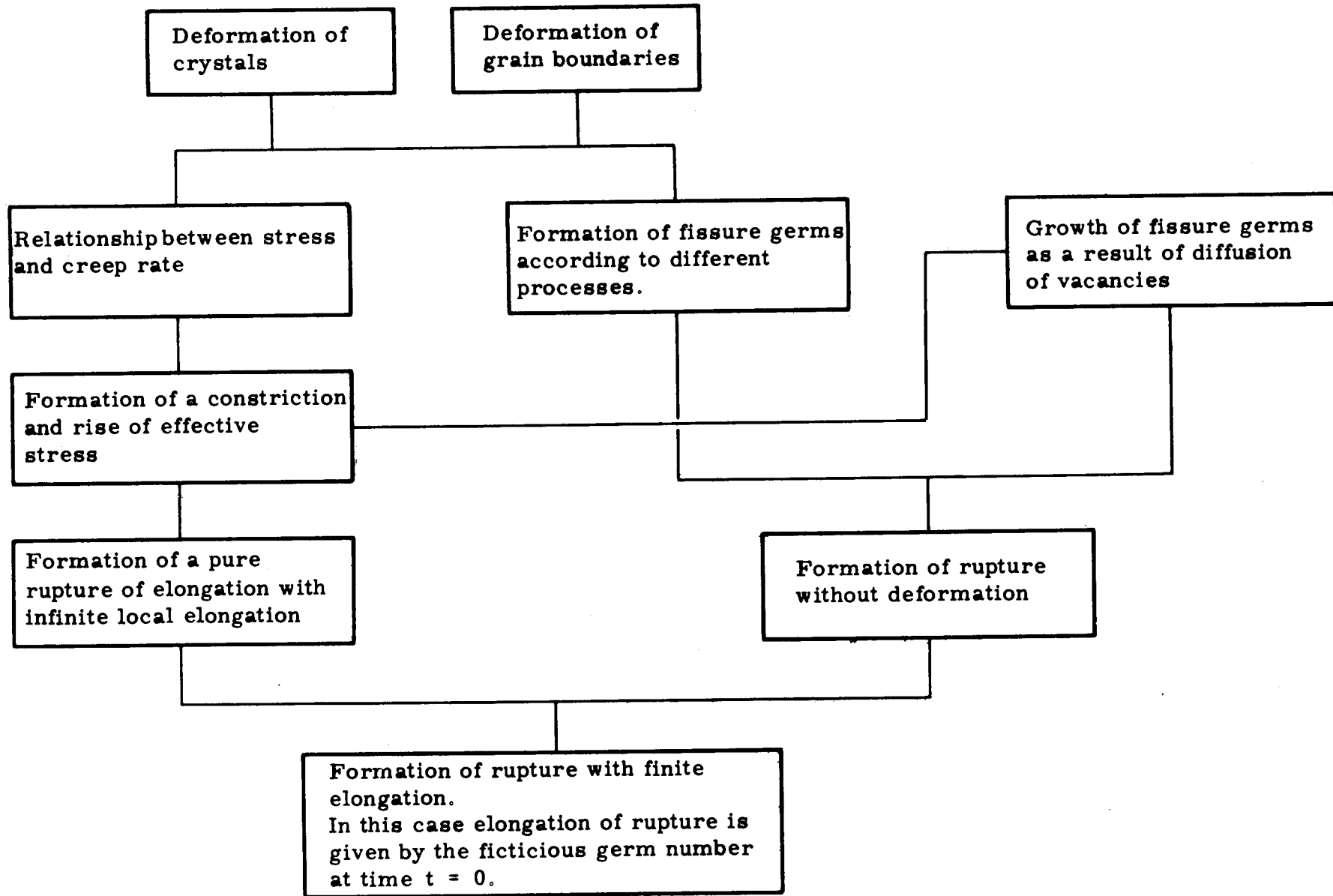


Fig. 4 - Schematic representation of the simplified model, based on the calculations.

Fig. 5 - Determining the creep law from the shape of the time-to-rupture curve (schematic).

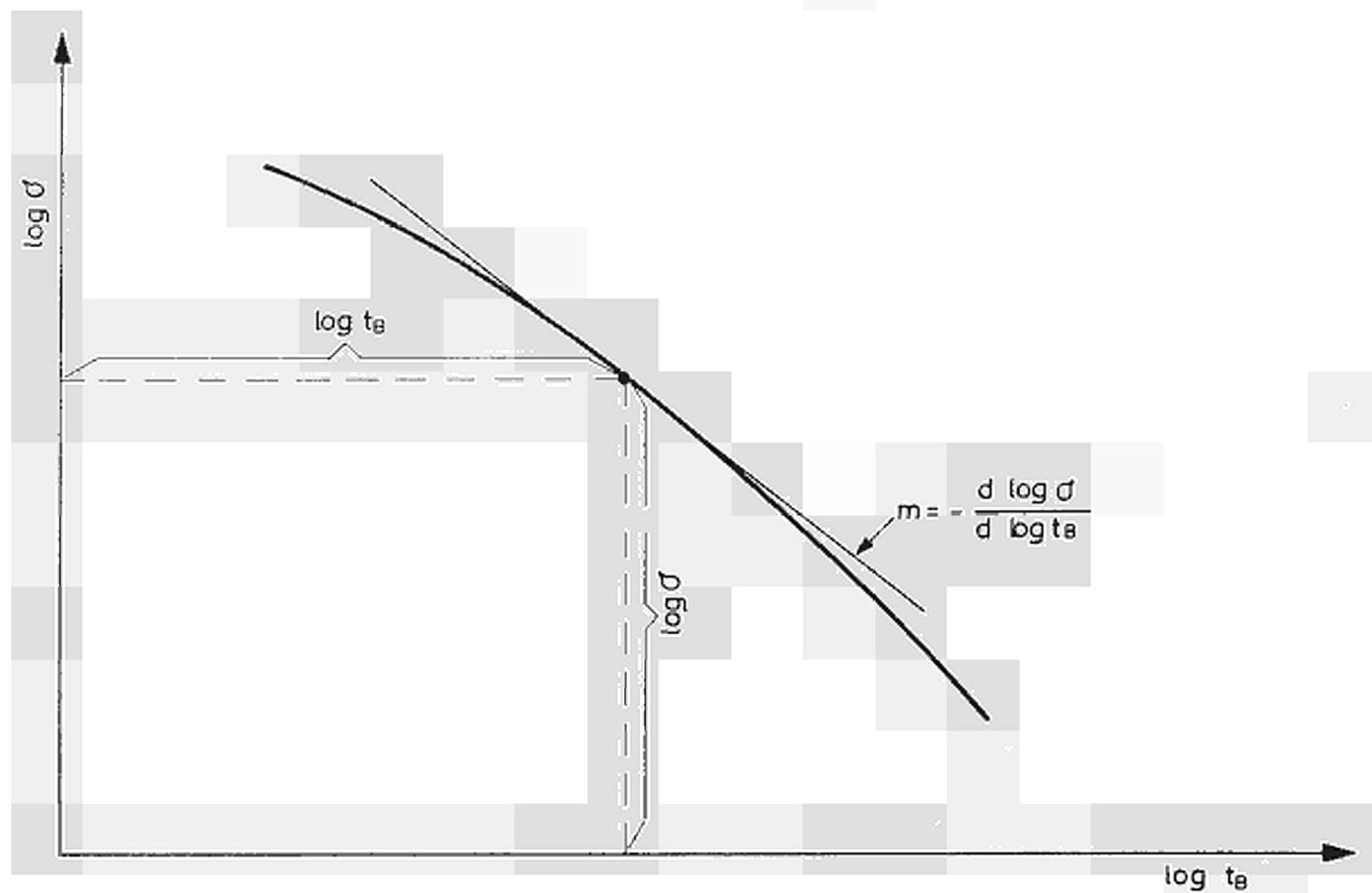


Fig. 6 - Change of time-to-rupture curves as a result of neutron irradiation for Cr - Ni - alloy No 1.

XH77T Ю P

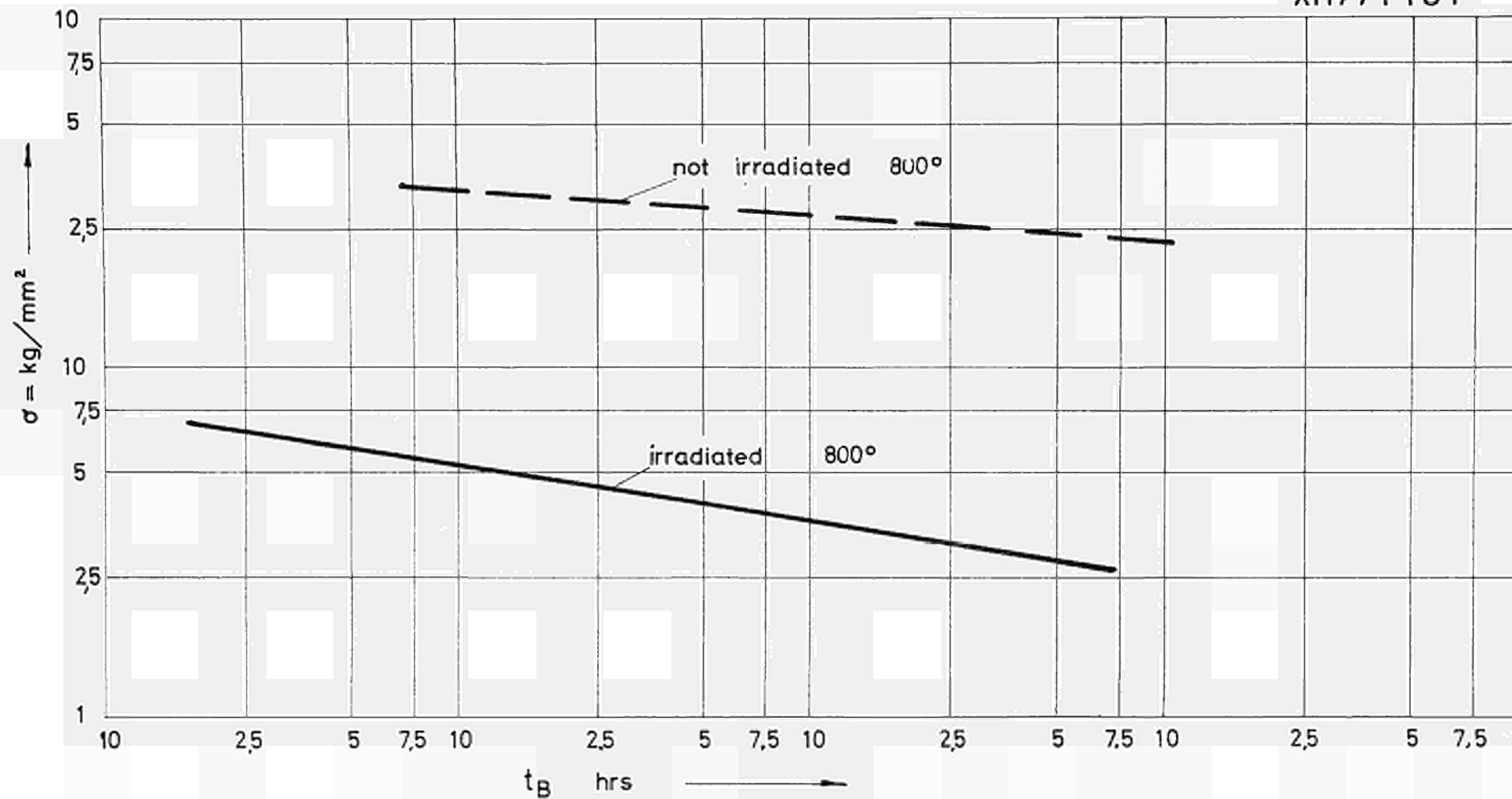


Fig. 7 - Slope of p as a function of t_B for time-to-rupture curves according to Fig. 6.

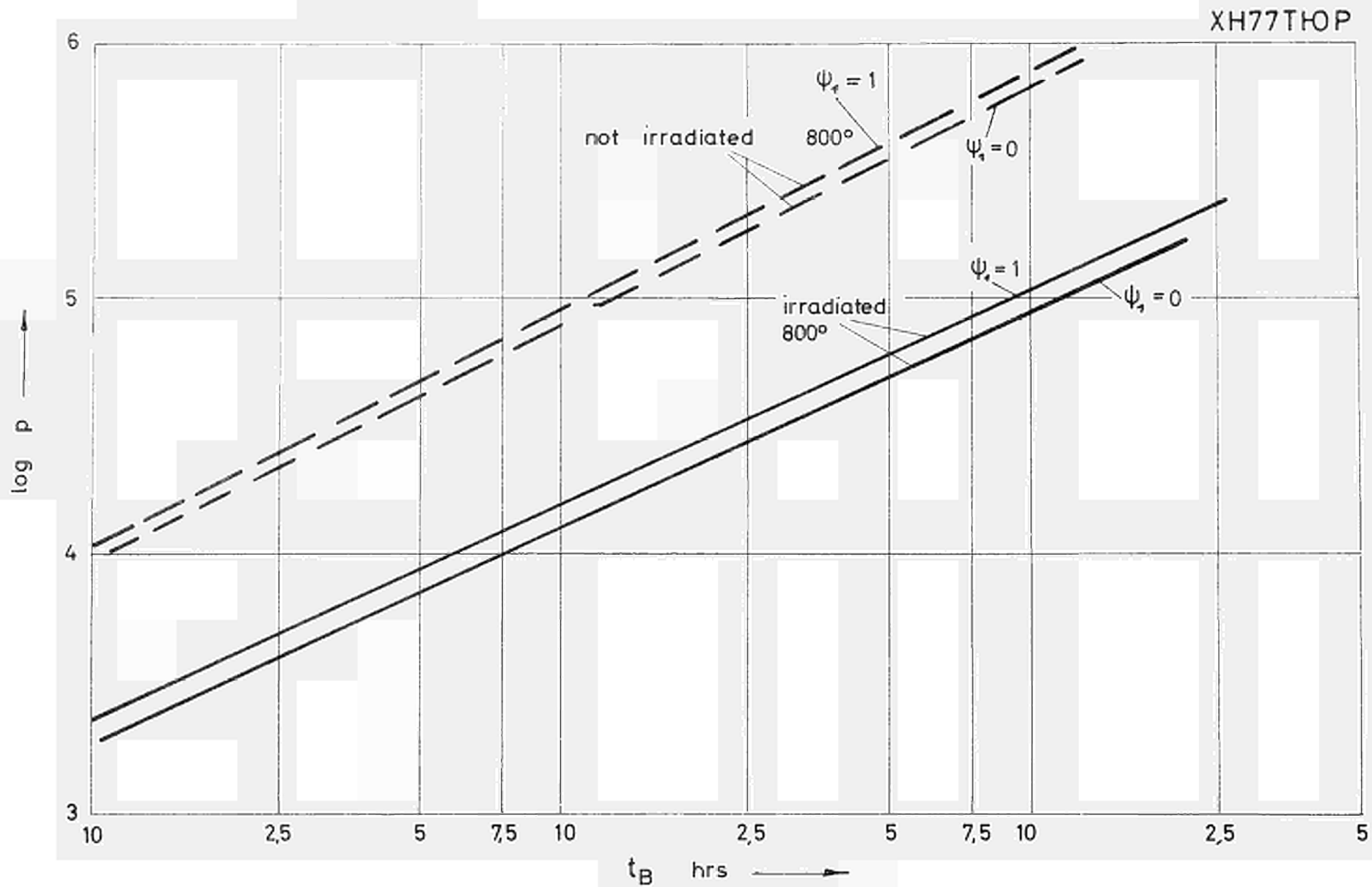


Fig. 8 - Change of time-to-rupture curves at 600° and 700°C by neutron irradiation for Cr - Ni - alloy No 2.

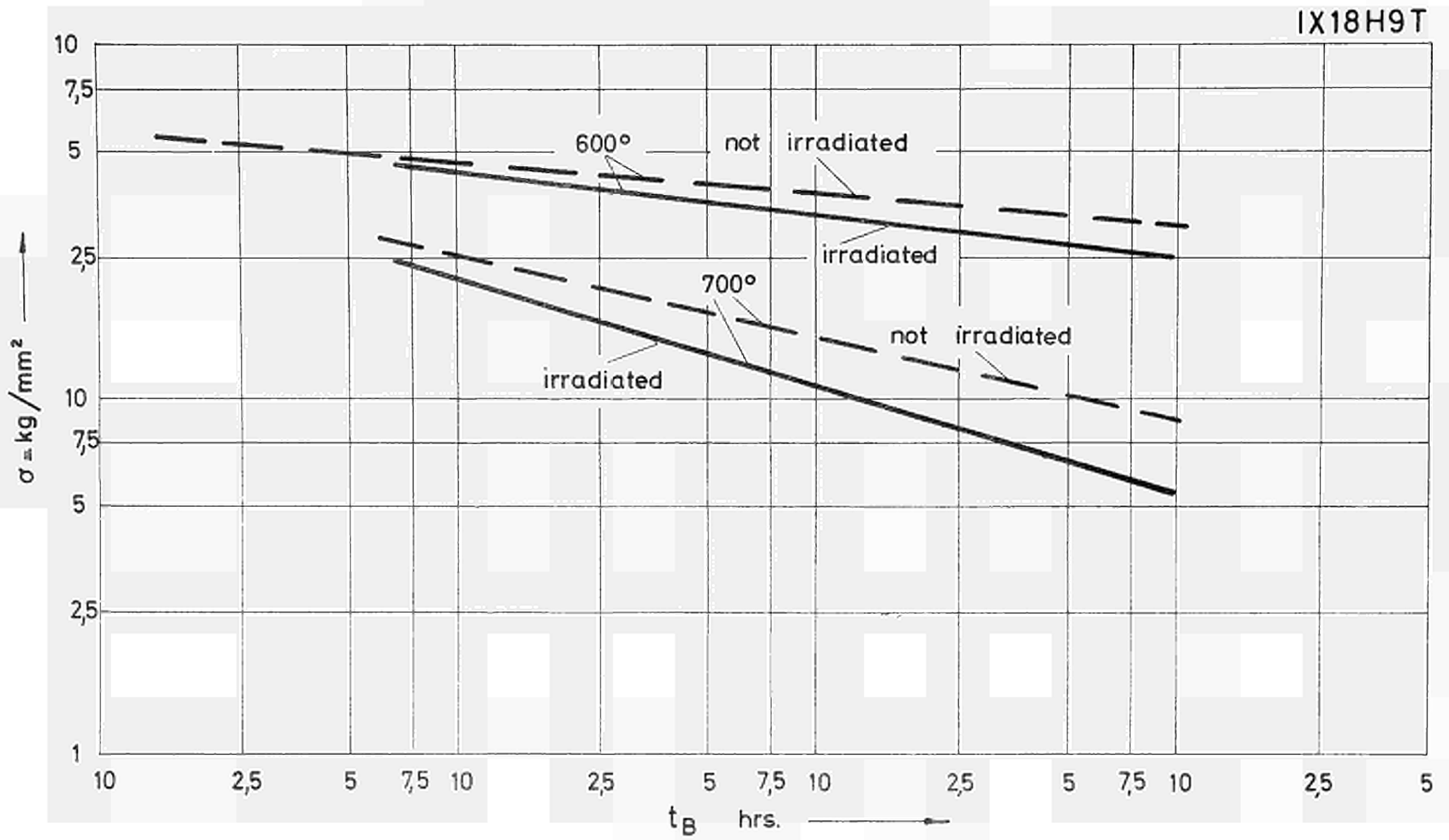


Fig. 9 - Slope of p as a function of t_B for time-to-rupture curves according to Fig. 8.

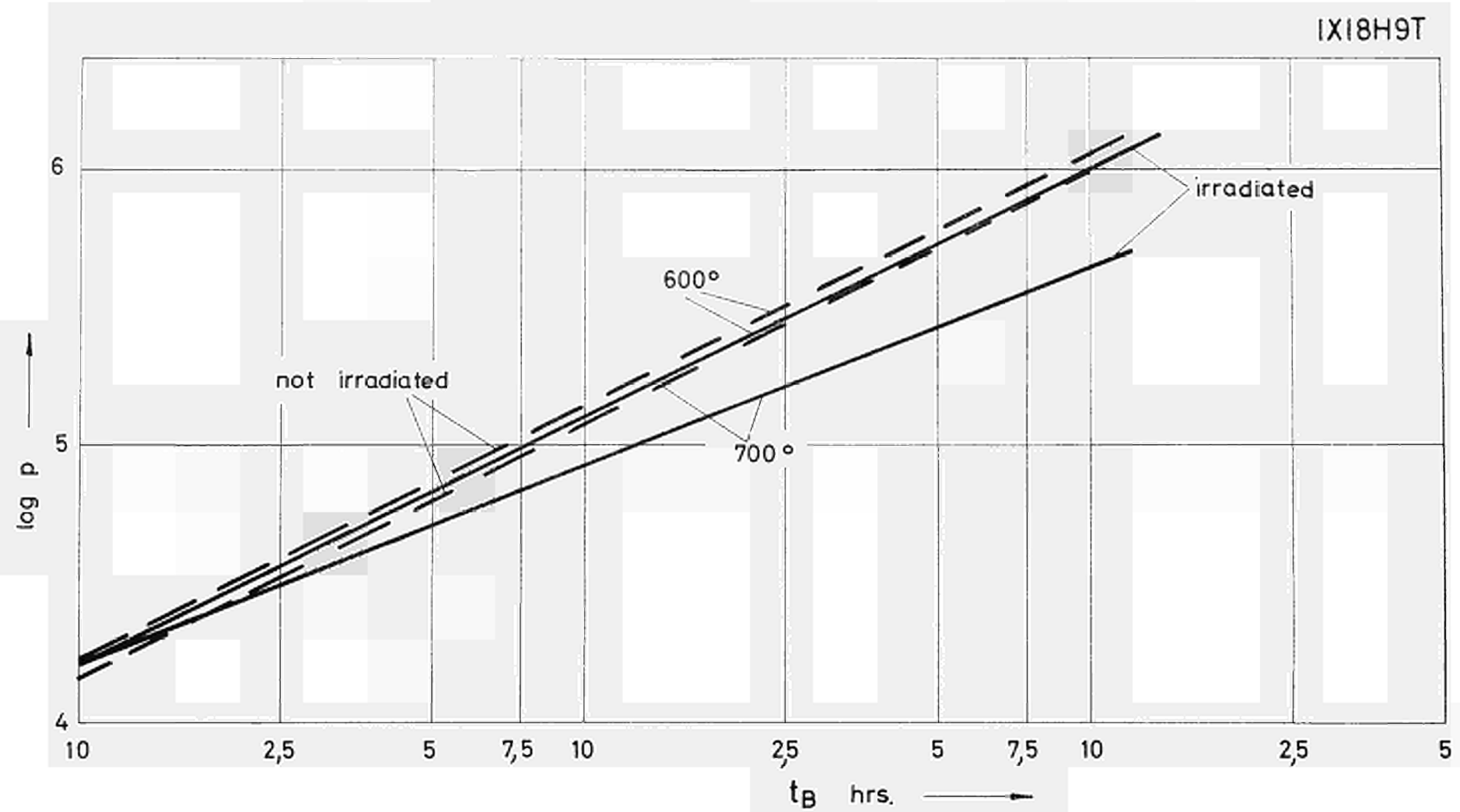


Fig. 10 - Change of time-to-rupture curves by neutron irradiation for steel type 304-stainless.

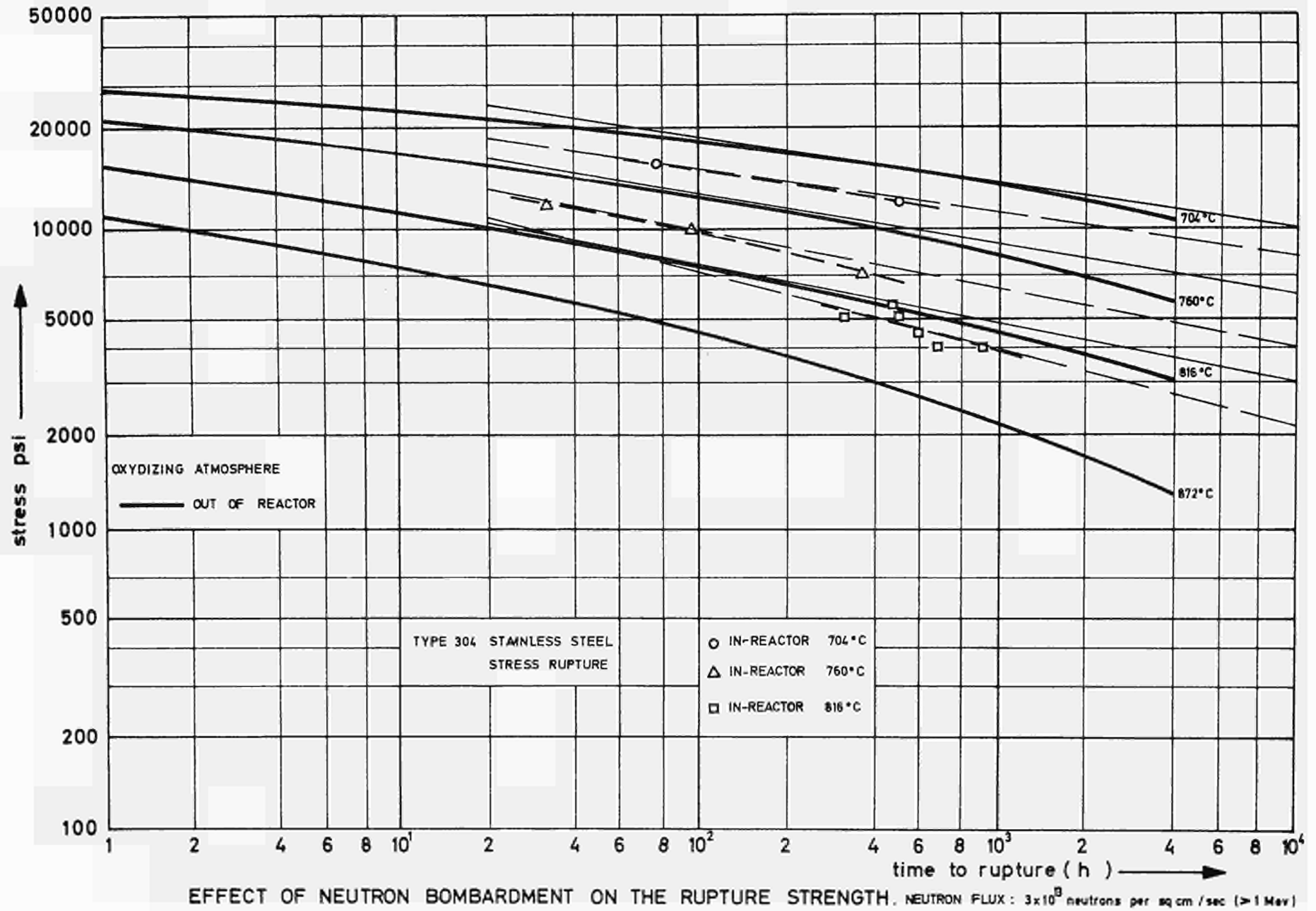


Fig. 11 - p/α as a function of t_B for time-to-rupture curves according to Fig. 10.

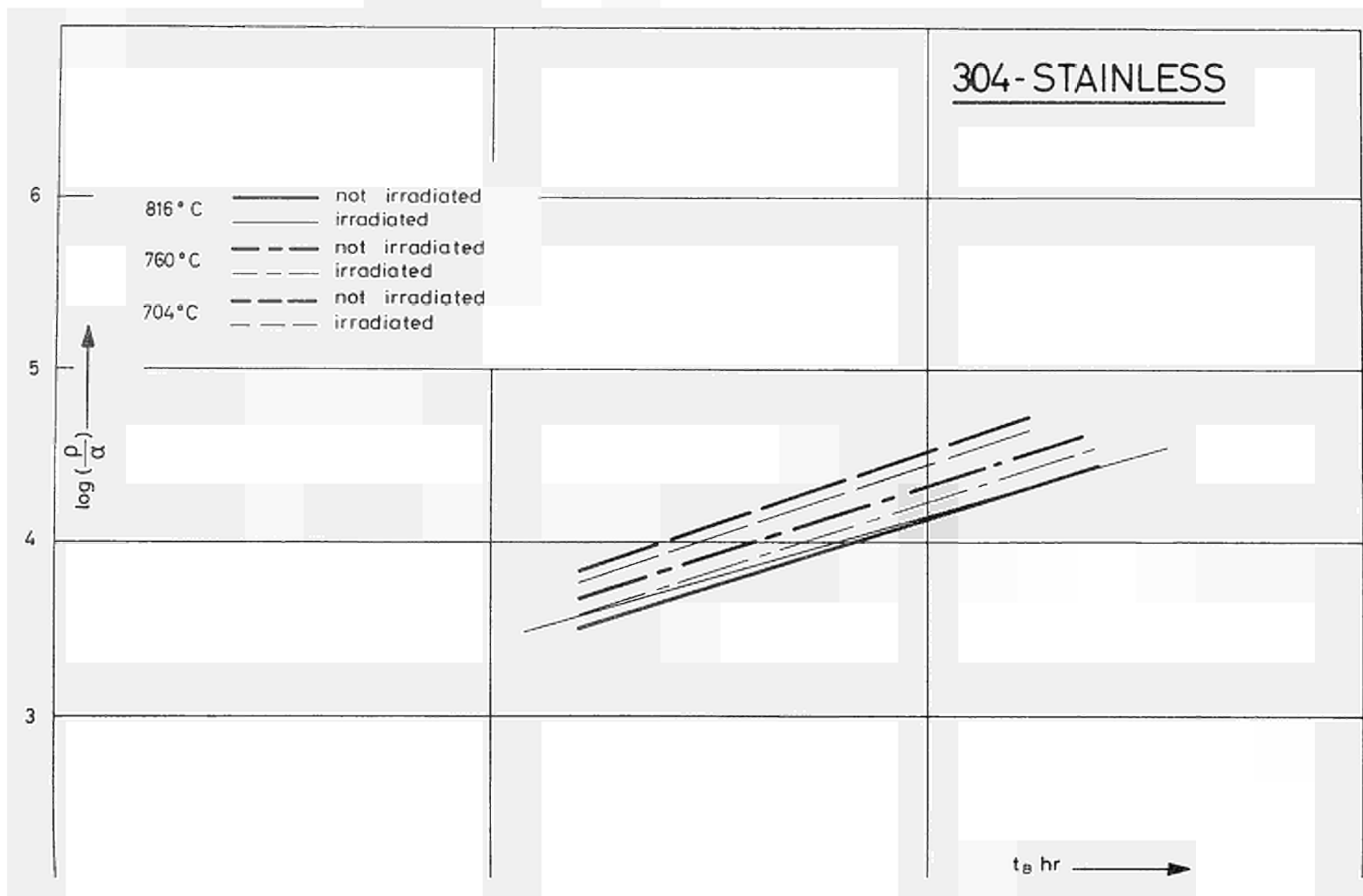


Fig. 12 - v_{sec} as a function of σ_0 for time-to-rupture curves according to Fig. 10.

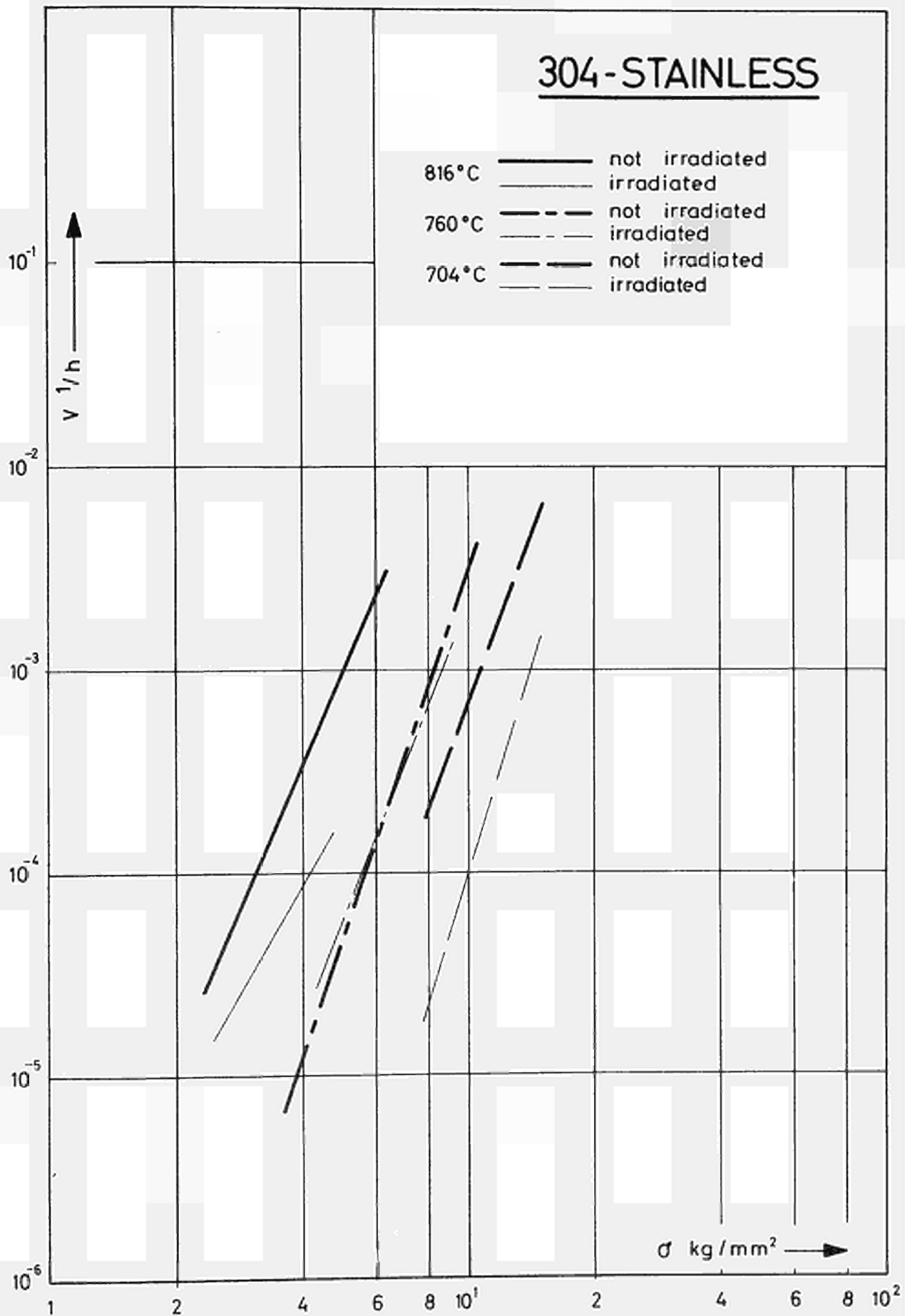


Fig. 13 - p/α as a function of v_{sec} for time-to-rupture curves according to Fig. 10.

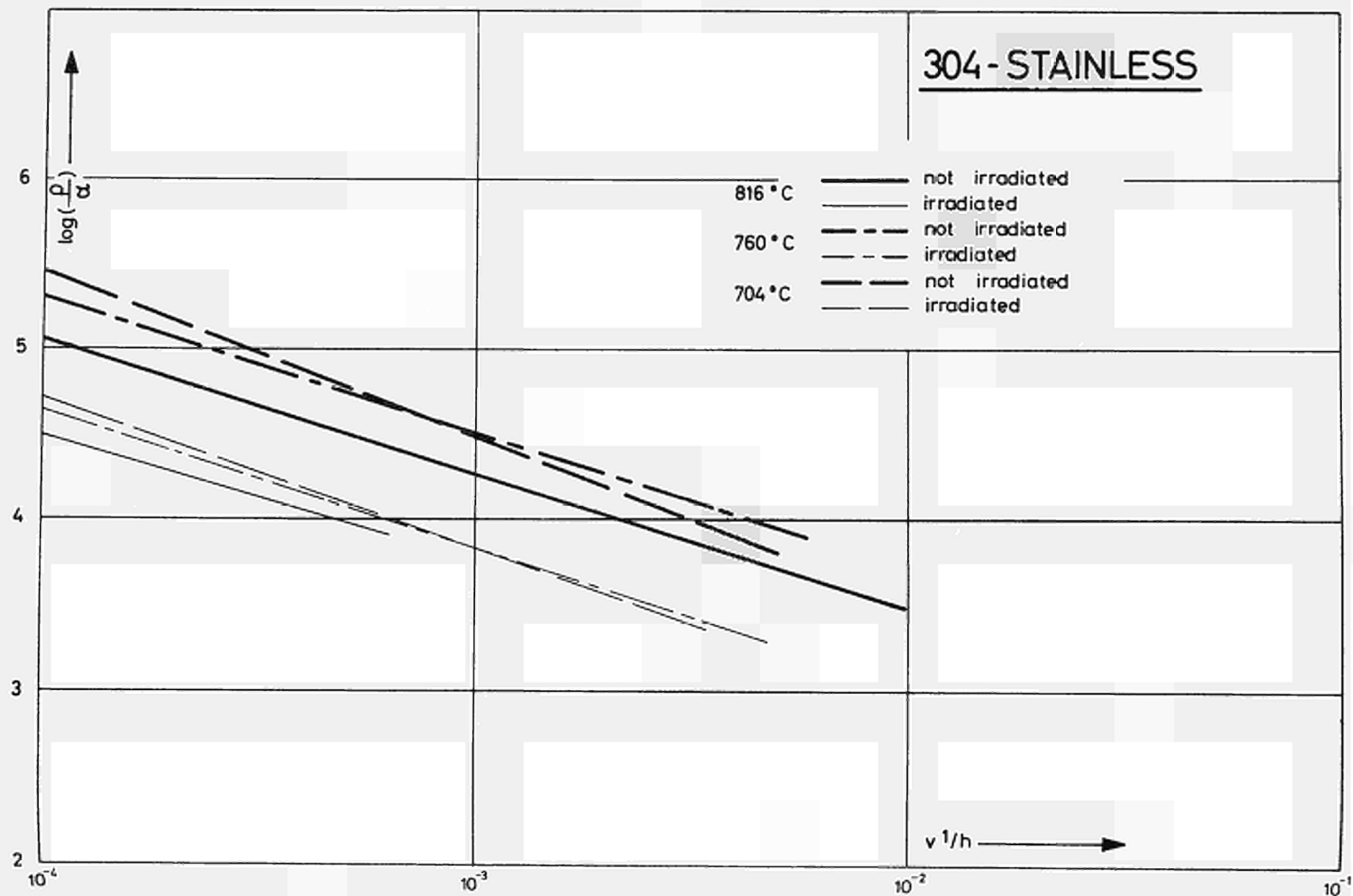


Fig. 14 - v^*/kT as a function of stress σ_0 for time-to-rupture curves according to Fig. 10.

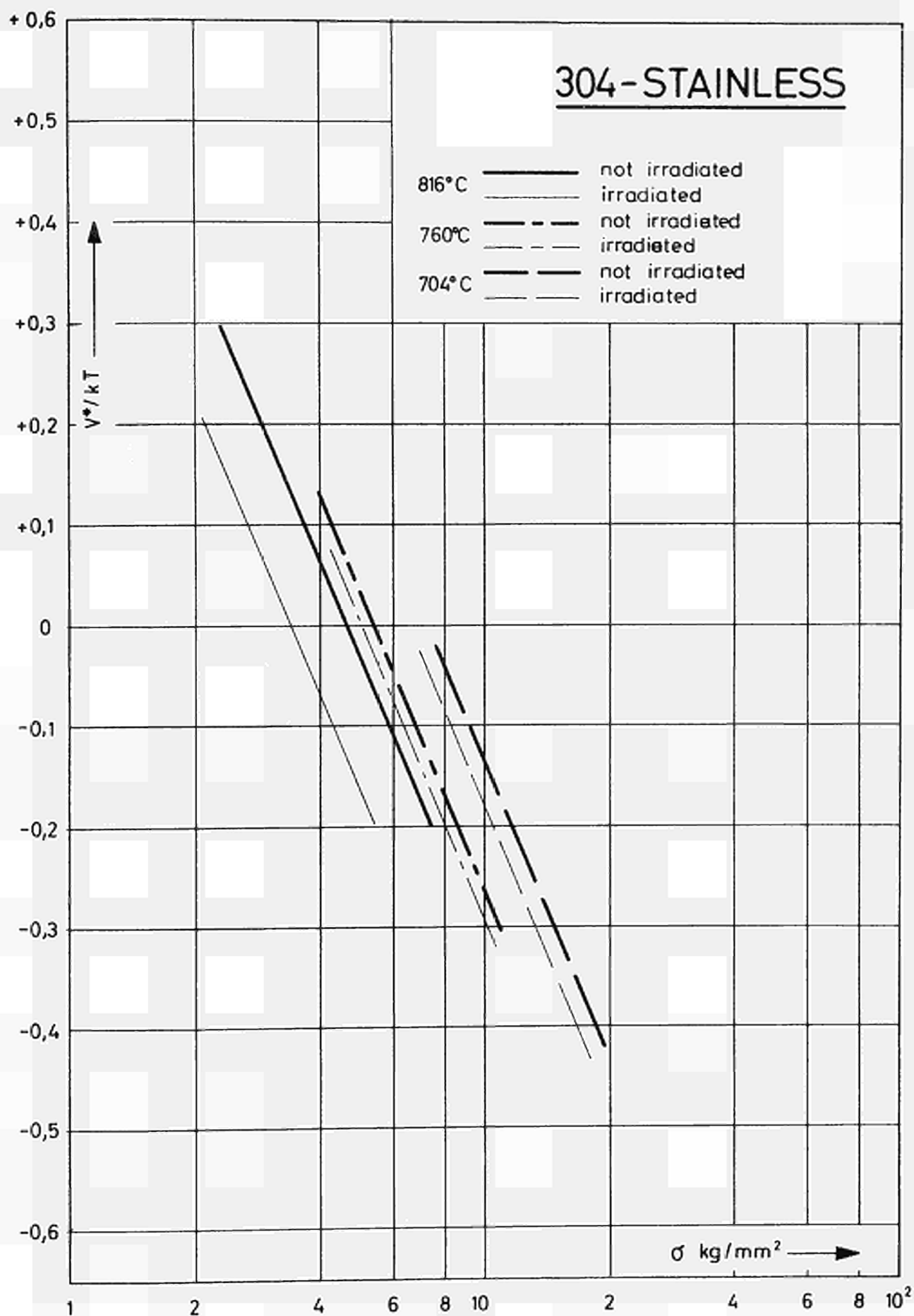


Fig. 15 - Time-to-rupture curve for Cr - Mo - V cast steel at 500°C.

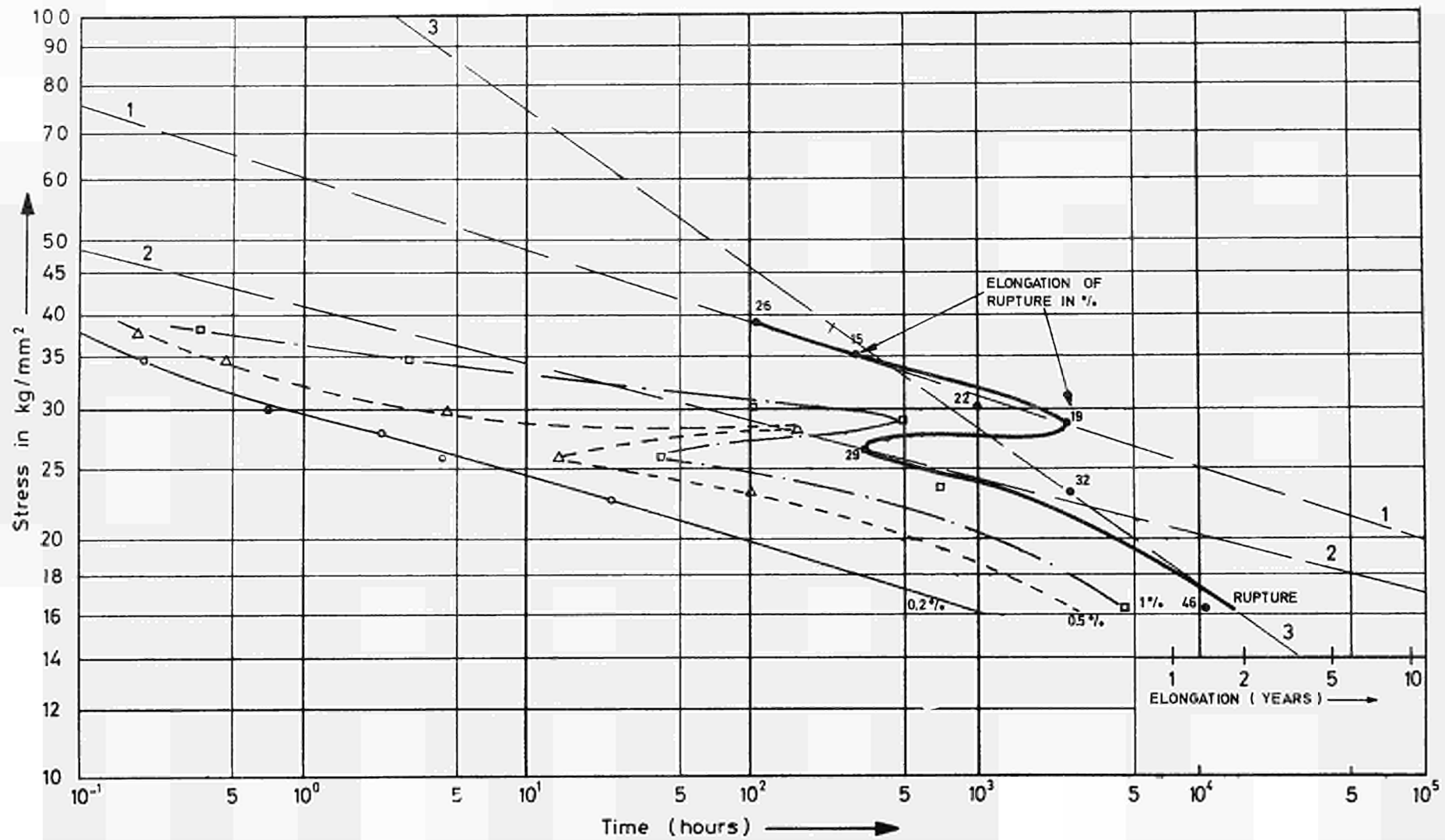


Fig. 16 - Slope of v_{sec} as a function of σ_0 for time-to-rupture curves according to Fig. 15.

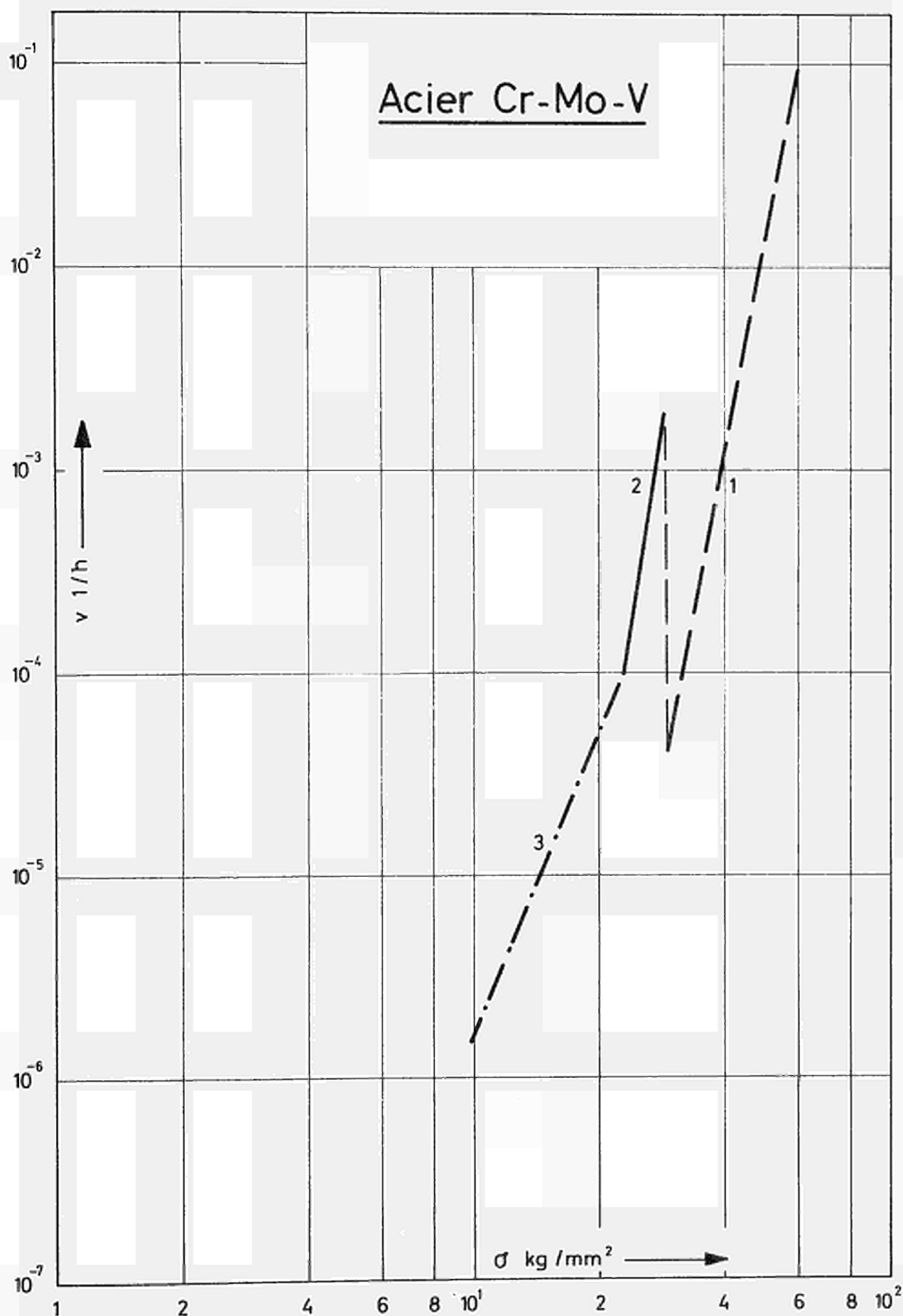


Fig. 17 - Slope of p/α as a function of σ_0 for time-to-rupture curves according to Fig. 15.

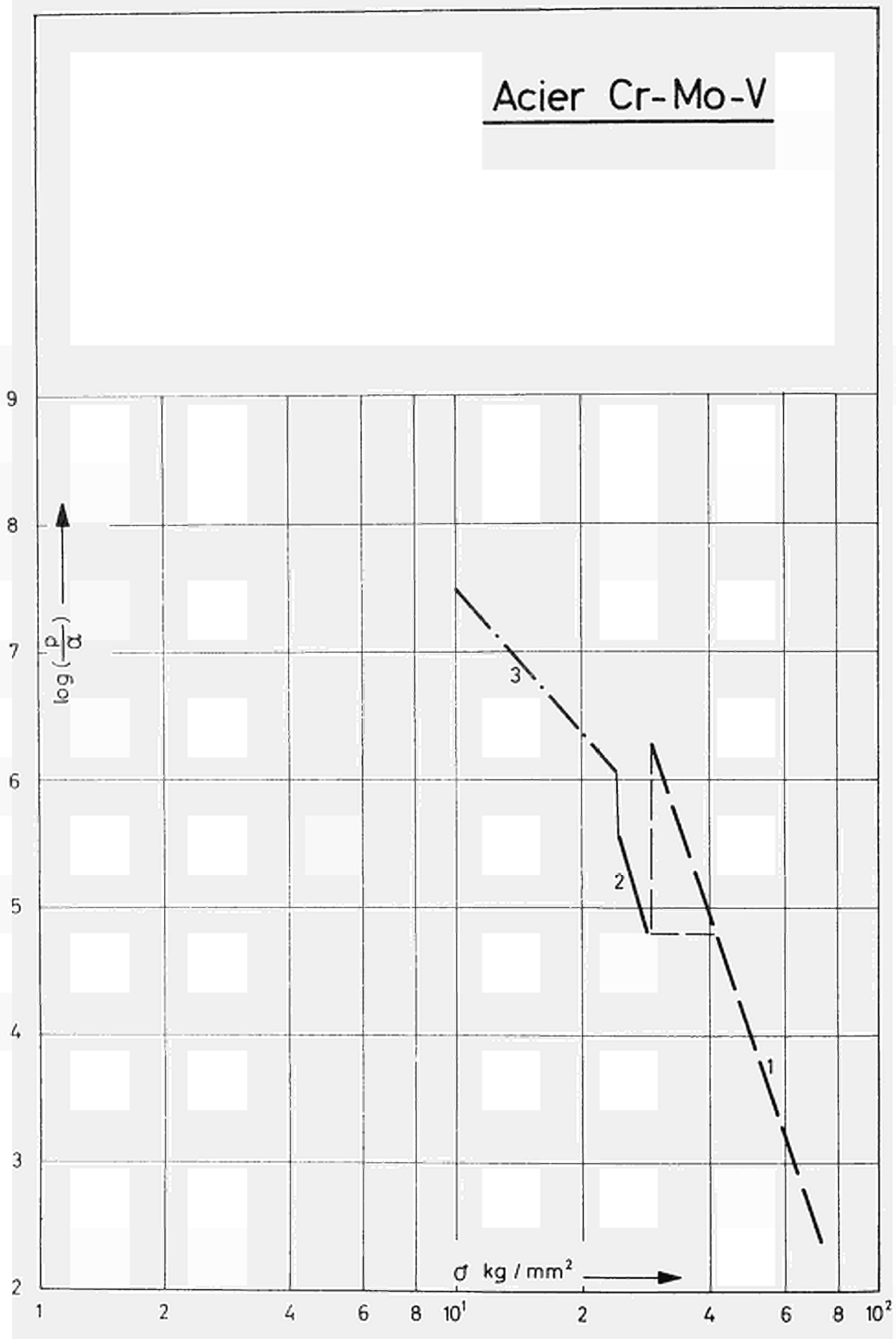


Fig. 18 - Slope of p/α as a function of v_{sec} for time-to-rupture curves according to Fig. 15.

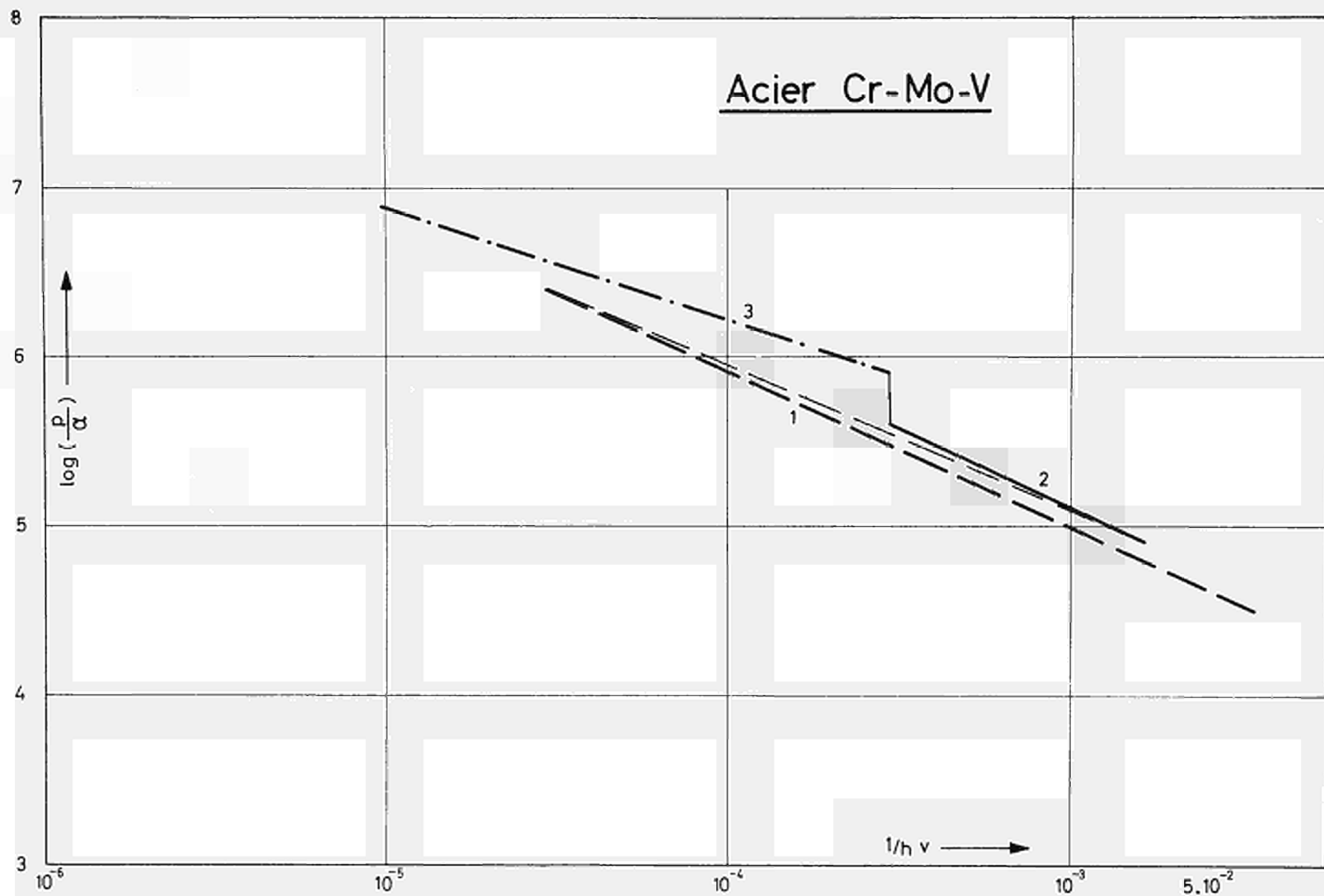


Fig. 19 - Slope of v^*/kT as a function of σ_0 for time-to-rupture curves according to Fig. 15.

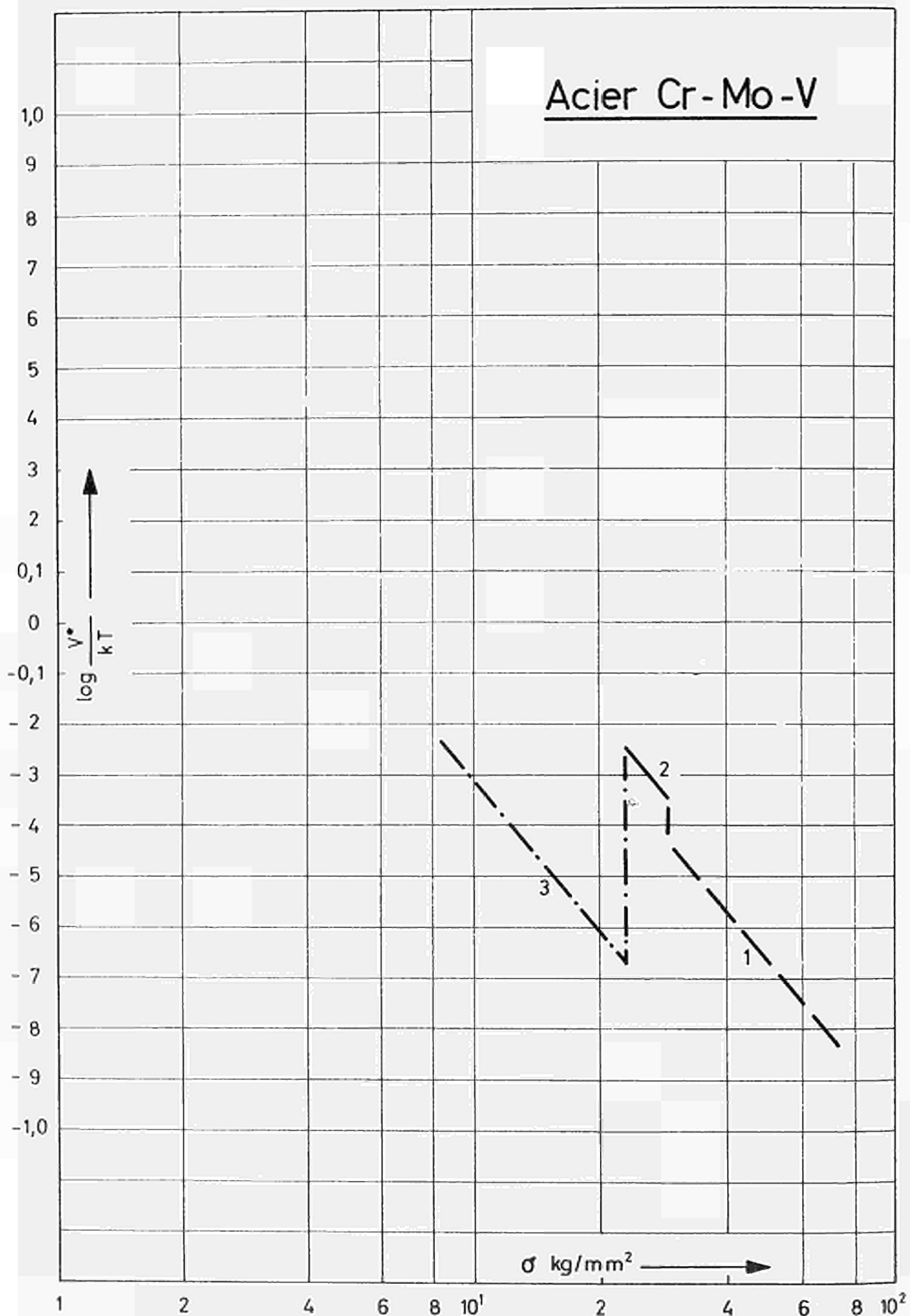


Fig. 20 - Results of time-to-rupture tests indicated by W.F. BROWN Jr., M.H. JONES, and D.P. NEWMAN, for a Cr-Mo-V-steel, represented in a double-logarithmic scale.

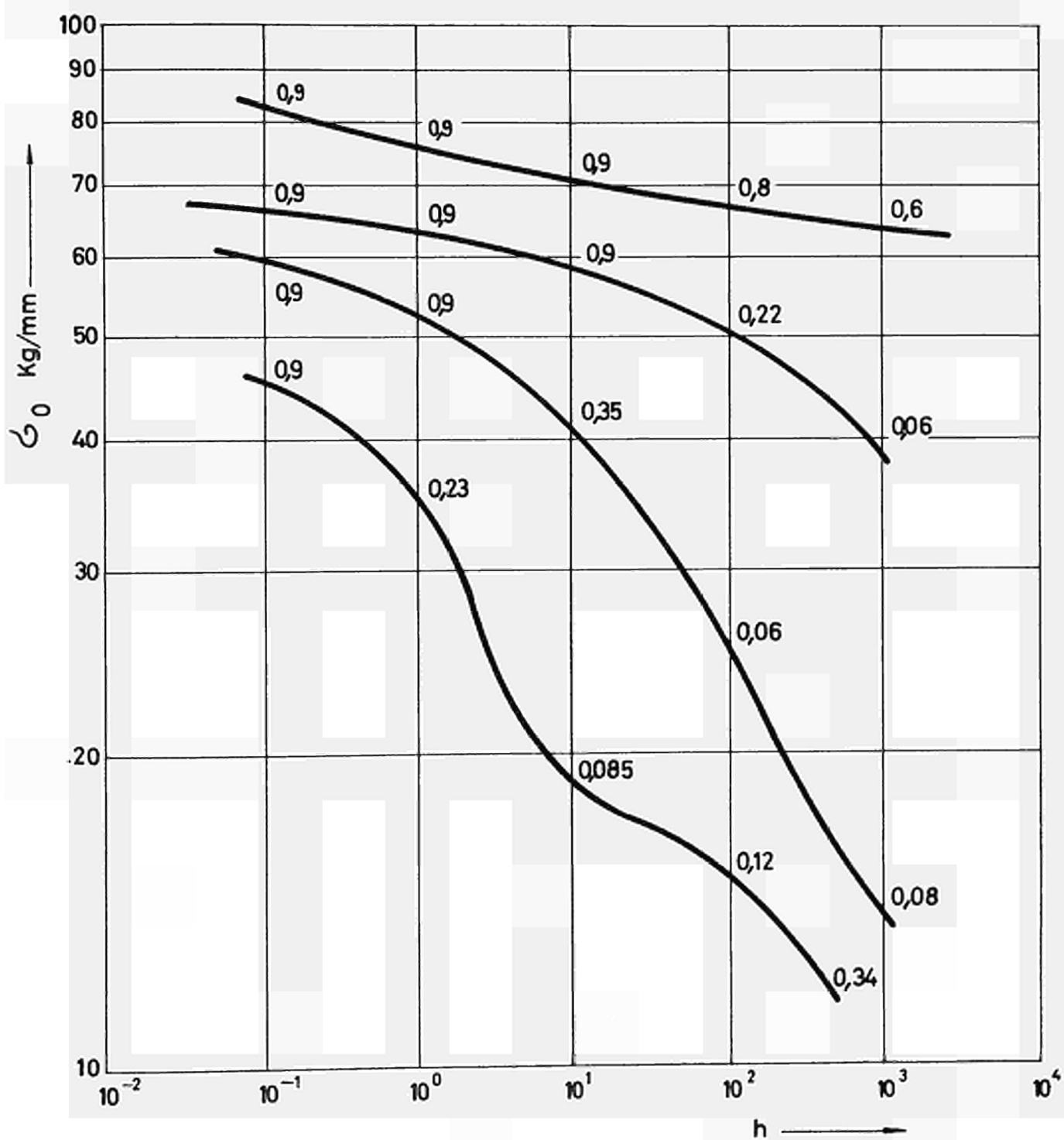


Fig. 21 - Values for local elongation, calculated from the reduction of area for the time-to-rupture tests mentioned in Fig. 20.

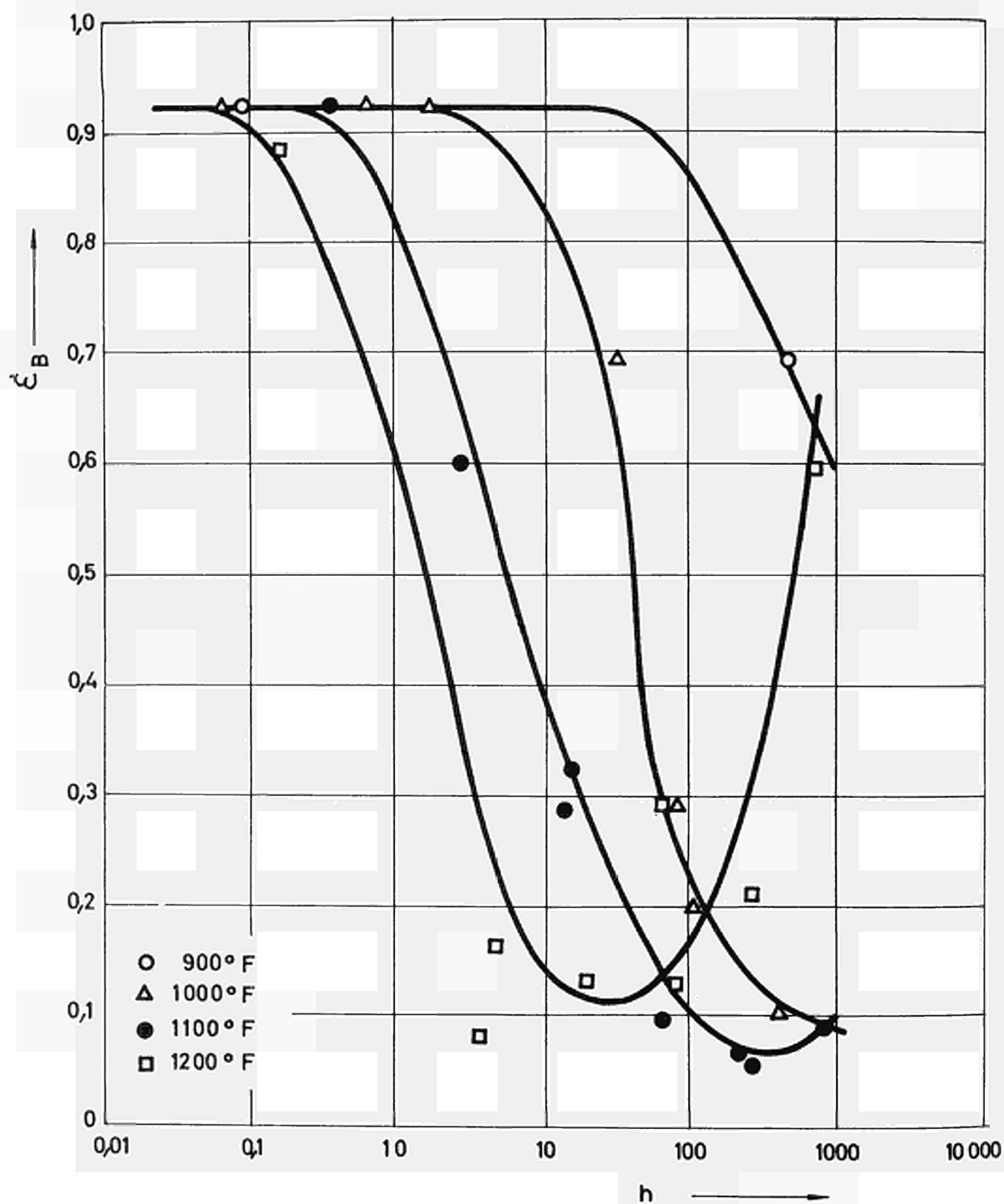


Fig. 22 - v_0 as a function of t_B for a Cr-Mo-V-steel.

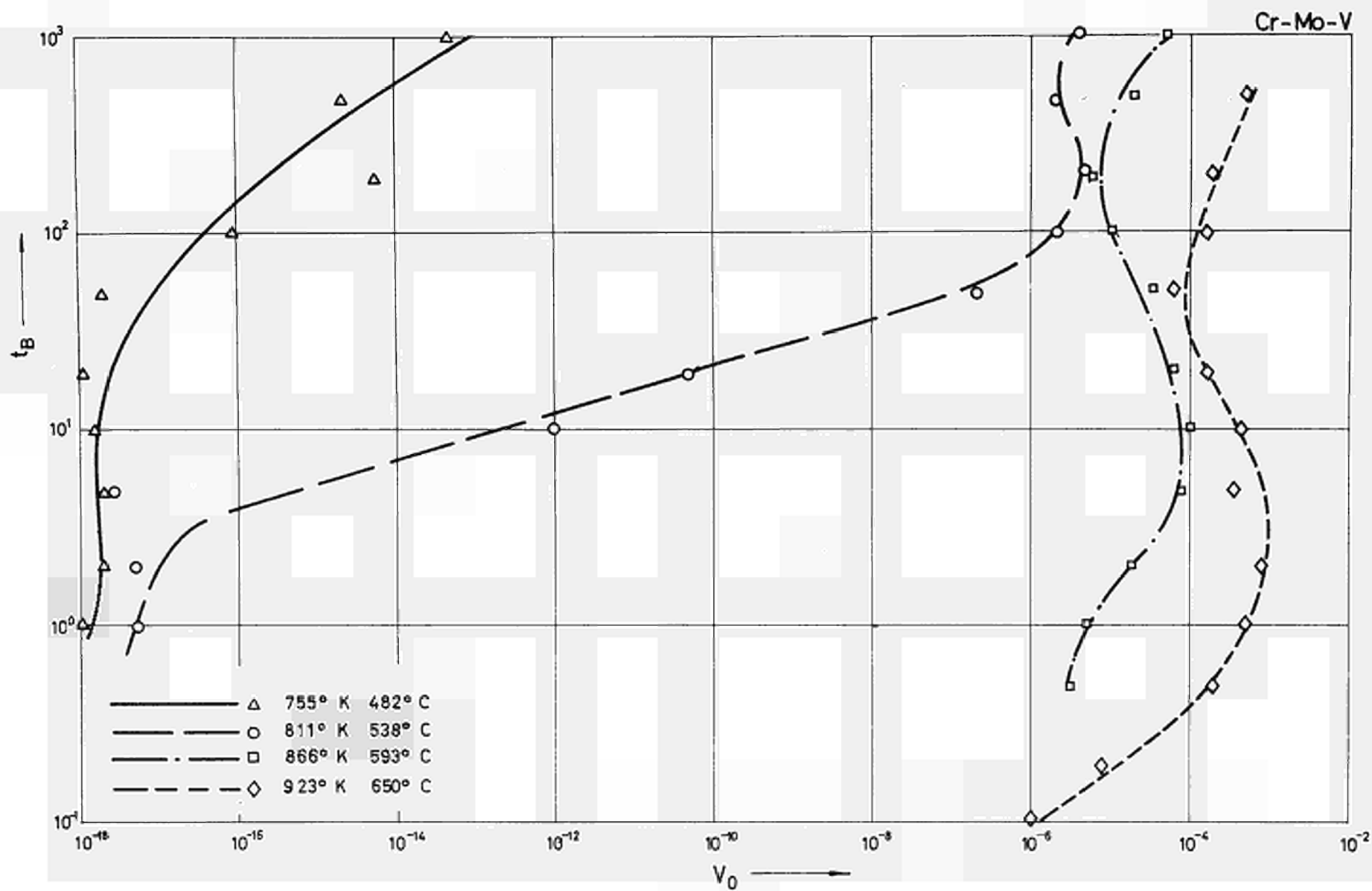


Fig. 23 - σ_1 as a function of t_B for a Cr-Mo-V-steel.

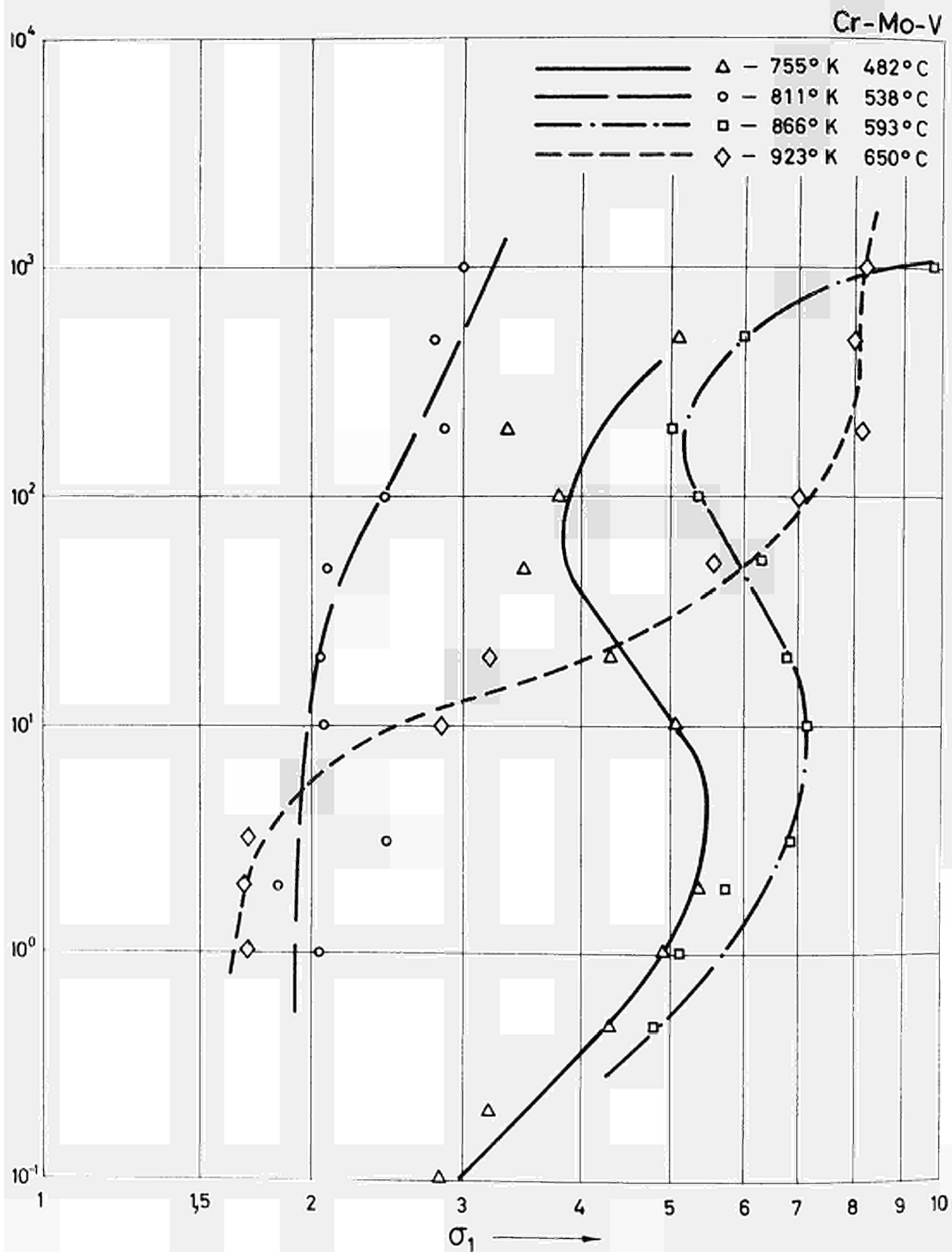


Fig. 24 - $\frac{\Delta H_1(T)}{2,3 RT} + \log v_0$ as a function of $\frac{\Delta H_3(T)}{2,3 RT} - \log t_B$ for a Cr-Mo-V-steel.

Cr-Mo-V

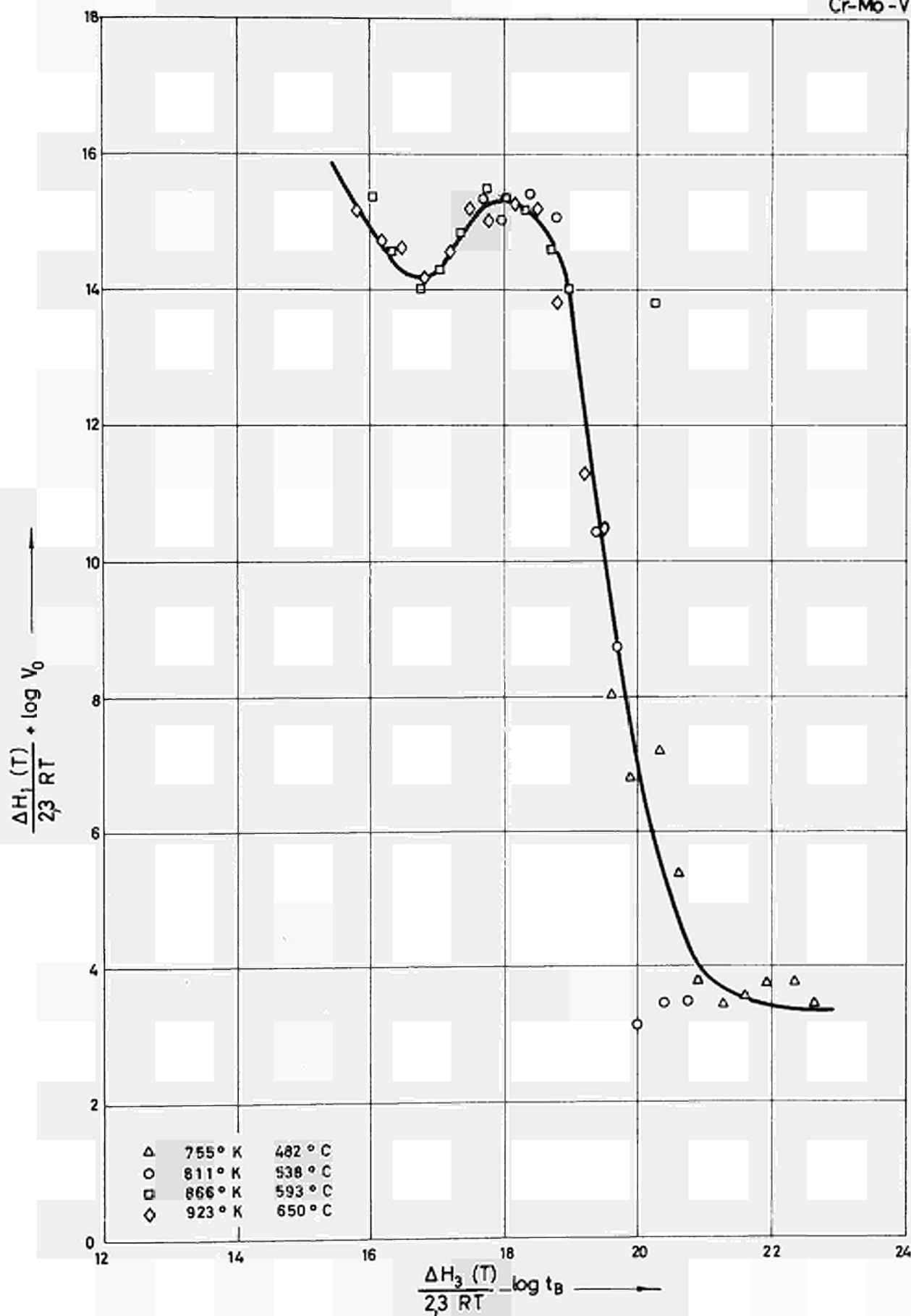
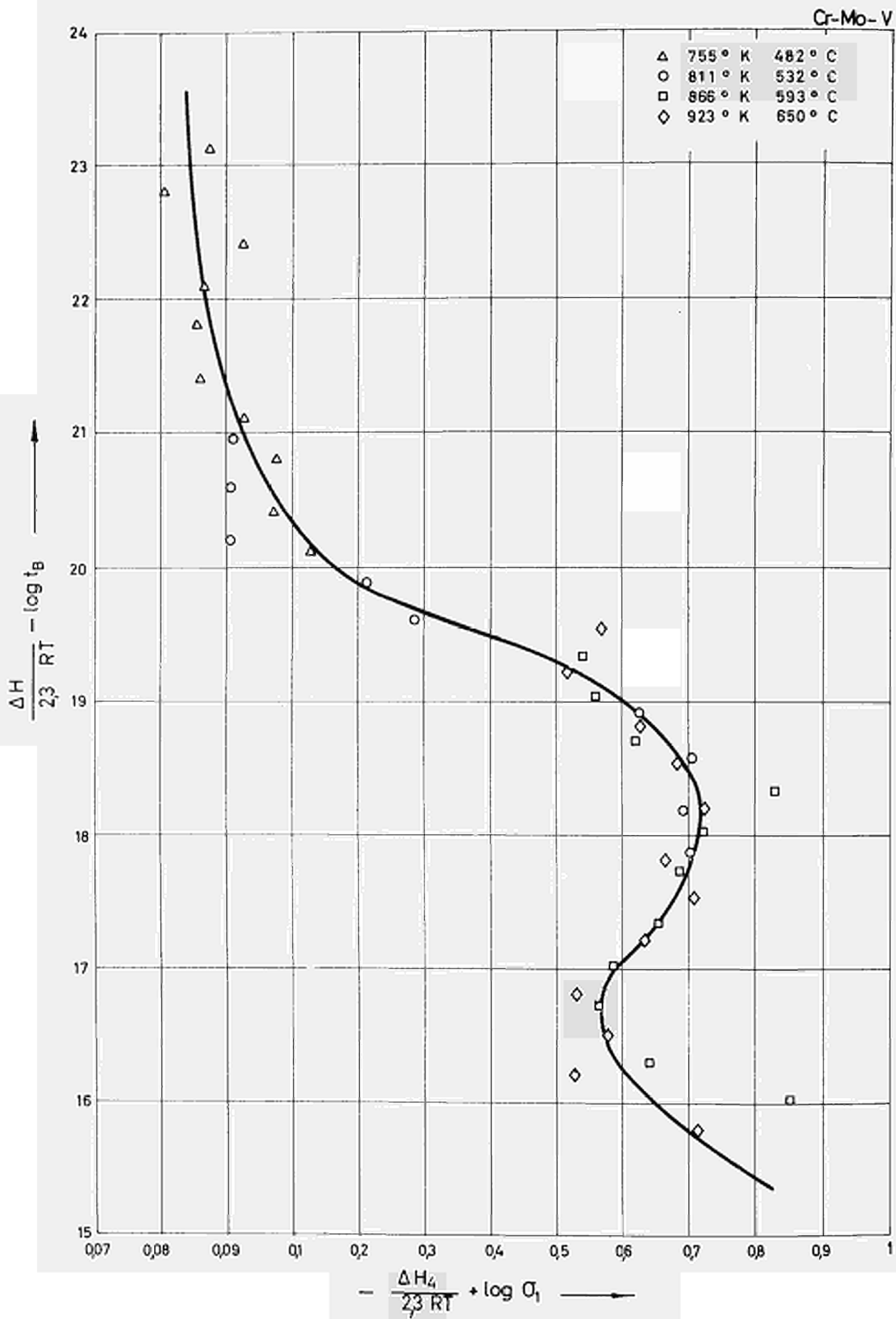


Fig. 25 - $\frac{\Delta H}{2,3 RT} - \log t_B$ as a function of $-\frac{\Delta H_4}{2,3 RT} + \log \sigma_1$
for a Cr-Mo-V steel.



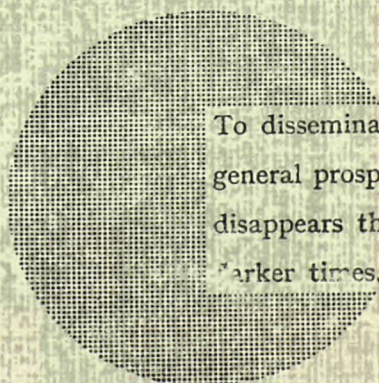
NOTICE TO THE READER

All Euratom reports are announced, as and when they are issued, in the monthly periodical **EURATOM INFORMATION**, edited by the Centre for Information and Documentation (CID). For subscription (1 year : US\$ 15, £ 5.7) or free specimen copies please write to :

Handelsblatt GmbH
"Euratom Information"
Postfach 1102
D-4 Düsseldorf (Germany)

or

Office central de vente des publications
des Communautés européennes
2, Place de Metz
Luxembourg



To disseminate knowledge is to disseminate prosperity — I mean general prosperity and not individual riches — and with prosperity disappears the greater part of the evil which is our heritage from darker times.

Alfred Nobel

SALES OFFICES

All Euratom reports are on sale at the offices listed below, at the prices given on the back of the front cover (when ordering, specify clearly the EUR number and the title of the report, which are shown on the front cover).

OFFICE CENTRAL DE VENTE DES PUBLICATIONS DES COMMUNAUTES EUROPEENNES

2, place de Metz, Luxembourg (Compte chèque postal N° 191-90)

BELGIQUE — BELGIË

MONITEUR BELGE
40-42, rue de Louvain - Bruxelles
BELGISCH STAATSBLAD
Leuvenseweg 40-42, - Brussel

LUXEMBOURG

OFFICE CENTRAL DE VENTE
DES PUBLICATIONS DES
COMMUNAUTES EUROPEENNES
9, rue Goethe - Luxembourg

DEUTSCHLAND

BUNDESANZEIGER
Postfach - Köln 1

NEDERLAND

STAATSDRUKKERIJ
Christoffel Plantijnstraat - Den Haag

FRANCE

SERVICE DE VENTE EN FRANCE
DES PUBLICATIONS DES
COMMUNAUTES EUROPEENNES
26, rue Desaix - Paris 15^e

UNITED KINGDOM

H. M. STATIONERY OFFICE
P. O. Box 569 - London S.E.1

ITALIA

LIBRERIA DELLO STATO
Piazza G. Verdi, 10 - Roma

EURATOM — C.I.D.
51-53, rue Belliard
Bruxelles (Belgique)

CDNA03752ENC